This document was prepared in conjunction with work accomplished under Contract No. DE-AC09-96SR18500 with the U. S. Department of Energy.

DISCLAIMER

This report was prepared as an account of work sponsored by an agency of the United States Government. Neither the United States Government nor any agency thereof, nor any of their employees, makes any warranty, express or implied, or assumes any legal liability or responsibility for the accuracy, completeness, or usefulness of any information, apparatus, product or process disclosed, or represents that its use would not infringe privately owned rights. Reference herein to any specific commercial product, process or service by trade name, trademark, manufacturer, or otherwise does not necessarily constitute or imply its endorsement, recommendation, or favoring by the United States Government or any agency thereof. The views and opinions of authors expressed herein do not necessarily state or reflect those of the United States Government or any agency thereof.

This report has been reproduced directly from the best available copy.

Available for sale to the public, in paper, from: U.S. Department of Commerce, National Technical Information Service, 5285 Port Royal Road, Springfield, VA 22161,
phone: (800) 553-6847,
fax: (703) 605-6900
email: orders@ntis.fedworld.gov
online ordering: http://www.ntis.gov/help/index.asp

Available electronically at http://www.osti.gov/bridge
Available for a processing fee to U.S. Department of Energy and its contractors, in paper, from: U.S. Department of Energy, Office of Scientific and Technical Information, P.O. Box 62, Oak Ridge, TN 37831-0062,
phone: (865)576-8401,
fax: (865)576-5728
email: reports@adonis.osti.gov

WSRC-TR-2002-00294

Comparison of MTI and Ground Truth Sea Surface Temperatures at Nauru

Robert J. Kurzeja* and Malcolm M. Pendergast**

*** Savannah River Technology Center**
Westinghouse Savannah River Co.

**** MMP Enterprises**
Martinez. GA

Table of Contents

ABSTRACT

Surface water temperatures calculated from Multispectral Thermal Imager (MTI) brightness temperatures and the robust retrieval algorithm, developed by the Los Alamos National Laboratory (LANL), are compared with ground truth measurements at a warm water site in the tropical western Pacific. Temperatures calculated for eighty-eight (88) images are compared with water temperatures measured at Nauru at image time and with data from the National Atmospheric Administration (NOAA) buoy network.

The bulk water temperature from Nauru and ocean buoys were corrected for warm layer (diurnal) and cool skin effects before comparison with each other, and with the surface temperatures calculated with the robust algorithm.

The 88 MTI images were inspected manually to find areas in each of the three Sensor Chip Assemblies (SCA's) which were as cloud-free as possible. The mean temperature in these areas was then calculated from the water surface temperature images provided by the LANL, and then divided into 3 categories, depending on the presence of clouds. Each area comprised several hundred to several thousand pixels.

It was found that the root-mean-square difference between the temperature calculated with the robust algorithm and that from the Nauru and buoy data was ~1C for clear skies. This error is comparable to the MTI design specifications. An apparent hot bias was found in the center SCA (SCA1), which can be attributed to lower brightness temperatures in band L (8.0-8.4 microns). The lower brightness temperature is probably due to a different wavelength-dependence of its transmission filter compared to the other SCA's.

The RMS error of the MTI water temperatures increased to ~2C when all of the images were included in the comparison and a cold bias was noted which is attributed to contamination by (cooler) clouds.

The error in the MTI retrieval was unaffected by the amount of water vapor in the atmosphere or the time of the image. In fact, the accuracy of the retrieved temperatures improved slightly as the mission progressed.

1. Introduction

This report evaluates MTI–derived surface water temperature near the tropical Pacific island of Nauru. The MTI sea-surface temperatures were determined by the Los Alamos National Laboratory based on the 'robust retrieval' (Tornow and Borel, 1994 and Tornow et al, 1994). An important advantage of the Nauru location is the relative uniformity of the sea-surface temperature and the tropical atmosphere. As a consequence, sea-surface temperature measurements at a single location can be applied with confidence to most areas of the MTI image. Moreover, the temporal variability in atmospheric temperature and water vapor is smaller than in other areas of the world and thus variability in MTI radiances can be attributed mostly to sea surface temperature variability. MTI-derived temperatures for cold water targets will be discussed in another report.

2. Methodology

The analysis consisted of two parts. In the first part available bulk water temperature data in the Pacific near Nauru at MTI image times were assembled and compared to assess their accuracy and consistency. The bulk water temperatures were then adjusted to determine the sea-surface temperature at the time of the MTI images. In the second part, the MTI Nauru images were inspected to identify the optimum (cloud-free) areas in each SCA (Sensor Chip Assembly) for each image. The water surface temperatures calculated by the Los Alamos National Laboratory with the 'robust water surface temperature' algorithm were compared with ground truth data after stratification based on the presence of clouds.

3. Calibration History

The calibration history of the MTI was discussed by Atkins et al. (2001). They asserted that the 1% design accuracy in the IR bands had probably been achieved after launch but noted variability in the brightness temperature between the three SCA's of up to ~0.5C for uniform sea-water targets in bands K and L. They argued that this variability was probably caused by uncertainty in the individual SCA filter functions, especially at short wavelengths, and was not due to radiometric differences. Thus, the brightness temperature of the SCA's would be expected to vary from scene to scene and Atkins et al. estimated this effect to be ~0.5C for band L.

On Oct 31, 2001 the MTI Telescope and Calibration Control Unit (TCAL) experienced a power failure. This shut down the optical assembly operational heaters (with a ~28C decrease in temperature), and caused the loss of the secondary mirror focus adjustment, door assembly, black body panel, visible panel, and quick calibration wheel assembly. After this failure, the calibration sequence was replaced by two deep-space looks. Periodic moon looks and ground calibration are being used to monitor changes in performance.

The quality of the MTI radiances, particularly in the IR, grew worse after the Oct 31 TCAL failure and greater offsets between the SCA's and linear variations in radiance across individual SCA's were observed. These have been attributed to thermally-induced mechanical shifts in the optics. This problem has been corrected by viewing targets with the satellite rotated by 90 degrees, i.e., viewing the same area with all pixels in each SCA. Differences between the SCA's have been corrected by normalizing SCA's 2 and 3 to the high end of SCA2, which also improved consistency with SCA1. Variations in radiance within SCA's have been corrected with 90 degree looks at uniform ocean targets.

The loss of the black body panels also precludes non-linear corrections in the radiance values and calibration of individual pixels. These corrections were maintained as before the TCAL failure.

In summary, Atkins et al. (2001) estimated a degradation in the inferred surface temperatures of 0.5-3.0C in brightness temperatures after the TCAL failure, with more specific estimates reserved for a later date.

4. Robust Algorithm

The MTI product evaluated in this report is called the Robust Water Surface Temperature, WST-R, referred to as WST in this report . This product was supplied to SRTC by the Los Alamos National Laboratory, and consists of a single band image with a resolution of 20 m. The values are floating point and in degrees Kelvin. The WST algorithm utilizes several sets of coefficients that are applied to Top-of-Atmosphere Brightness temperatures, TOAB, of MTI bands J, K, L, M and N as a function of the Zenith-to-MIT angle. TOAB values can be generated internally within the algorithm or obtained as one of the MTI products and the angle, Zenith2MTI, is obtained from the MTI image header text file. Table 1 shows WST coefficients for daytime and nighttime developed by Tornow and Borel (1994) which are based upon LOWTRAN simulations for 380 different atmospheres. Although both nadir and backward looks can be used to calculate robust temperatures, only the nadir look has been used in this study.

Table 1. Coefficients for calculating WST from Top-of-Atmosphere brightness temperatures of MTI thermal bands for Zenith-to-MTI angles ranging from 0 to 40 degrees. (provided by William B. Clodius, LANL 1/28/02)

Fit	Terms	D/N	Angle	SCA	Offset	J	K	L	M	N
Lowtran	KLMN	D	0	All	5.743		0.33212	-3.14438	1.90504	1.87483
Lowtran	KLMN	D	5	All	5.795		0.33412	-3.15406	1.91016	1.87715
Lowtran	KLMN	D	10	All	5.939		0.3399	-3.18222	1.92495	1.88404
Lowtran	KLMN	D	15	All	6.21		0.40727	-3.40041	2.0104	1.94887
Lowtran	KLMN	D	20	All	6.609		0.42151	-3.46828	2.04266	1.96835
Lowtran	KLMN	D	25	All	7.176		0.44035	-3.55667	2.07981	1.99808
Lowtran	KLMN	D	30	All	7.937		0.46456	-3.66945	2.12558	2.03733
Lowtran	KLMN	D	35	All	8.959		0.49464	-3.80867	2.17788	2.08942
Lowtran	KLMN	D	40	All	10.307		0.52892	-3.96954	2.23235	2.15537
Lowtran	JKLMN	N	0	All	14.843	1.96669	0.64702	-1.52437	-3.54234	3.37936
Lowtran	JKLMN	N	5	All	14.935	1.97006	0.64843	-1.52463	-3.55321	3.3853
Lowtran	JKLMN	N	10	All	15.214	1.98006	0.65252	-1.52509	-3.58573	3.40298
Lowtran	JKLMN	N	15	All	15.131	2.01508	0.66721	-1.54074	-3.6149	3.39894
Lowtran	JKLMN	N	20	All	15.82	2.03828	0.67662	-1.54024	-3.69419	3.44213
Lowtran	JKLMN	N	25	All	16.763	2.06801	0.68817	-1.53823	-3.79702	3.49761
Lowtran	JKLMN	N	30	All	17.987	2.10568	0.70295	-1.53484	-3.92863	3.56809
Lowtran	JKLMN	N	35	All	19.572	2.15121	0.72076	-1.52952	-4.0911	3.65506
Lowtran	JKLMN	N	40	All	21.543	2.20745	0.73866	-1.51156	-4.28701	3.75045

LANL determines coefficients for a specific Zenith-to-MTI angle by interpolation from adjacent angles. SRTC has developed regression equations to provide coefficients as a function of Zenith-to-MTI angle for ease of incorporating the WST computation within an Excel spreadsheet and/or an ENVI band math expression. Equation (1) and (2) give $TDAY_{WST}$ and $TNITE_{WST}$ for daytime

and nighttime respectively, where A is the zenith-to-MTI angle and TOABi are brightness temperatures for MTI band "i". All temperatures are in degrees Kelvin.

$$TDAY_{WST} = (0.003547*A^2 - 0.03283*A+5.8330) + (0.000027*A^2 + 0.004071*A+0.32116)*TOAB_K + (-0.000237*A^2 - 0.011829*A-3.11275)*TOAB_L + (0.000072*A^2 +0.005715*A+1.8901)*TOAB_M + (0.00012*A^2 - 0.002243*A+1.86854)*TOAB_N$$

$$TNITE_{WST} = (0.0005894*A^2 - 0.07613*A+15.0502) + (0.000124*A^2 + 0.001082*A+1.9640)*TOAB_J + (0.000042*A^2 + 0.000679*A+0.64521)*TOAB_K + (0.000054*A^2 - 0.002085*A-1.51868)*TOAB_L + (-0.000551*A^2 +0.003844*A-3.55281)*TOAB_M + (0.000306*A^2 - 0.003158*A+3.38763)*TOAB_N$$

$TDAY_{WST}$ and $TNITE_{WST}$ use the same coefficients for the three SCA's, despite known biases between the SCA's. Thus, one result from this study is to document the magnitude of these biases.

5.0 Ground truth data

Ground truth near Nauru was obtained from three sources: (a) the DOE ARM site on the island, (b) water temperature measurements at a depth of 10 cm at MTI image time near a jetty on the west side of the island, (c) the network of oceanic buoys operated by NOAA. Water temperatures measurements near Nauru were obtained for ~30% of the MTI images through a cooperative agreement between SRTC and Nauru ARM support personnel. These measurements were obtained with small, automatically recording temperature sensors (Tidbits, Section 5.1a) which were cast into deep water from the end of the jetty and then slowly reeled back in. On a few occasions additional data were collected from a boat several hundred meters from the shore. Finally, the NOAA oceanic buoy temperatures (1 meter depth) are available for nearly all MTI image times but these measurements are at least 200 km from Nauru (166.5E, 0.8S) and must be adjusted to find the sea-surface (skin) temperature.

There are several sources of uncertainty in the ground truth data which must be considered in addition to sensor error. These are the warm layer (diurnal) variations (buoys), cool skin effects (buoys and Tidbits), spatial variability (buoys), and island effects (Tidbits). These will be discussed in more detail in this section.

A complete listing of the data used in this report is given in Table 2. The specific column entries in this table will be discussed in later sections of this report.

Mo	DY	YR	D/N	SEQ	Proc	IM#	Tim	TB #	TB tm	Tbuc	TBc	DIUT	DCT	SKN	SP	B0N	DiUB	DCB	B2N/5S	SKN	WSC	WSG	Q-W	CSC	CSG	Q-C	ESC	ESG	Q-E
5	19	0	D	141	804	17045	140								4		0.4	29.37	28.97	29.17	297.9	0.4	1	302.2	0.4	1	301.1	0.3	1
6	10	0	D	197	804	18231	138								4.8		0.3	29.85	29.55	29.65									
7	2	0	D	274	804	20096	131							29.48	6.5		0.2	29.69	29.49	29.49	297.9	0.9	1	301.3	1.0	1	302.4	0.2	0
7	3	0	D	263	710	19774	140	313059	300	29.5	29.68			29.48	6.5		0.2	29.29	29.09	29.09	301.7	0.4	1	304.3	0.4	1	302.7	0.2	1
7	25	0	D	326	804	21630	130								2.5	29.37	1	30.37		30.17	301.0	0.3	0	303.5	0.2	0	301.8	0.2	1
8	5	0	D	366	804	22793	123								3	29.47	0.8	30.27		30.07	298.6	0.4	2	303.9	0.4	2	301.1	0.3	1
8	29	0	D	478	804	27009	120								1.8	29.39	1.5	30.89		30.69	300.3	0.4	2	302.0	0.4	2	300.8	0.3	2
8	30	0	D	485	804	27314	128								1.8	29.41	1.5	30.91		30.71	301.7	0.3	0	304.9	0.3	0	302.7	0.2	1
9	22	0	D	590	701	30034	112								2	29.48	1.7	31.18		30.98									
9	23	0	D	596	804	30185	120								3.5	29.59	0.6	30.19		29.99	302.1	0.4	1	304.4	0.3	1	302.3	0.2	2
10	5	0	D					313055	100	29.4	29.66			29.46	1.7	29.25	1.5	30.75		30.55									
10	6	0	D					313059	125	29.3	29.48			29.28	3	29.22	0.7	29.92		29.72									
10	17	0	D					313055	100	29.4	29.66			29.46	5.4	29.01	0.3	29.31		29.11									
10	18	0	D					313055	140	29.4	29.66			29.46	5	28.91	0.3	29.21		29.01									
11	1	0	D	757	803	33769	117								3.5	29.47	0.6	30.07		29.87	305.5	1.0	0	304.3	0.3	0	302.2	0.5	1
11	12	0	D					313059	200	29.2	29.38			29.18	4	28.99	0.4	29.39		29.19									
11	13	0	D					313055	120	29.1	29.36			29.16	4.5	29.04	0.4	29.44		29.24									
11	27	0	D	1072	804	100413	101								6	29	0.2	29.2		29	300.0	0.2	0	302.8	0.2	1	299.5	0.4	2
12	12	0	D	1140	710	100725	104								4.5	29.04	0.4	29.44		29.24	301.0	0.3	0	303.2	0.2	0	301.1	0.2	0
12	26	0	D	1208	803	101031	57								7	29.16				28.86	283.0	0.7	1	275.8	0.8	2	280.2	0.8	1
12	28	0	D	1216	803	101060	109	376339	120	29.8	29.80			29.50	4.7	29.21	0.3	29.51		28.91	300.4	0.3	1	302.8	0.1	1	300.3	0.2	2
1	11	1	D	1274	803	101259	59	376339	100	29.4	29.40			29.20	6.5	28.85	0.2	29.05		28.85	301.1	0.2	0	302.9	0.1	1	301.2	0.1	2
1	27	1	D	1340	703	101602	59								6	28.41	0.2	28.61		28.41	300.2	0.3	0	301.9	0.1	0	300.3	0.2	1
2	11	1	D	1413	801	101972	51	342122	100	29	29.01			28.81	6	28.21	0.2	28.41		28.21	296.3	0.4	2	298.8	0.1	1	298.7	0.6	1
2	12	1	D	1416	801	101983	57	342122	100	28.6	28.60			28.40	6.5	28.15	0.2	28.35		28.15	293.5	0.3	1	295.9	0.1	2	294.2	0.5	2
2	27	1	D	1474		102308	47								2	28.47	1.3	29.77		29.57	297.7	0.5	1	300.4	0.4	1	298.5	0.6	2
2	28	1	D	1479	710	102327	53								2	28.51	1.3	29.81		29.61									
3	16	1	D	1571	710	102871	47								6.5	28.42	0.2	28.62		28.42	300.6	0.3	1	302.9	0.1	2	300.8	0.2	2
4	21	1	D					376339	50	29.2	29.20			29.00	4		0.4	29.25	28.85	29.05									
4	22	1	D					313055	50	29.3	29.56			29.36	4		0.4	29.14	28.74	28.94									
4	23	1	D	1732	708	103786	51	342122	100	29.3	29.31			29.11	5		0.25	29.04	28.79	28.84	301.4	0.2	1	304.0	0.1	0	301.8	0.2	0
5	11	1	D	1820	705	104115	40								2.5		1	30.13	29.13	29.93	300.7	0.2	0	302.9	0.2	0	301.3	0.2	1
5	12	1	D	1825	705	104130	45								3		0.7	29.63	28.93	29.43	299.9	0.2	1	302.4	0.2	0	300.8	0.2	1
5	30	1	D	1891	704	104397	32								1.3		1.8	31.35	29.55	31.15			0			0			0
5	31	1	D	1893	704	104404	36								3.3		0.7	30.17	29.47	29.97	302.3	0.2	0	304.1	0.1	0	302.6	0.2	0
6	1	1	D	1899	704	104427	41								2		1.3	30.77	29.47	30.57	302.5	0.3	1	304.6	0.2	2	302.8	0.2	2
7	12	1	D	2103	704	105146	28	342122	100	30.3	30.31			30.11	2	29.68	1.3	30.98		30.78	302.5	0.4	0	305.0	0.3	0	303.0	0.2	0
7	13	1	D					342122	50	30.9	30.91			30.71	3	29.58	0.8	30.38		30.18									
8	3	1	D	2226	705	105612	24	313055	40	30.7	30.97			30.77	2	29.78	1.3	31.08		30.88	297.7	0.4	2	301.0	0.7	1	298.8	0.2	1
8	4	1	D	2232	705	105633	28								3	29.72	0.8	30.52		30.32	298.9	0.4	1	301.1	0.1	2	298.9	0.2	2
8	26	1	D	2364	705	106122	22								2	29.78	1.3	31.08		29.48	302.5	0.2	0	304.0	0.1	0	302.2	0.2	2
8	27	1	D	2369	705	106141	26								2	29.85	1.3	31.15		30.95	303.5	0.2	1	304.7	0.1	1	303.0	0.2	1
9	18	1	D	2478	708	106636	16								3.5	30.45	0.6	31.05		30.85	303.9	0.2	0	305.7	0.2	0	303.7	0.2	1
9	19	1	D	2485	708	106655	19								3.5	30.46	0.6	31.06		30.86	303.1	0.3	0	304.6	0.1	0	302.8	0.2	1
10	14	1	D	2600	710	107170	11								2	30.05	1.3	31.35		31.15	303.1	0.3	0	303.7	0.2	1	301.7	0.3	2
10	15	1	D	2603	710	107182	14								2	30.18	1.3	31.48		31.28	303.5	0.4	1	305.8	0.2	0	303.6	0.2	1
10	16	1	D	2610	710	107204	0								2	30.09	1.3	31.39		31.19	303.4	0.3	1	305.4	0.2	1	303.7	0.2	2
7	1	0	N					313059	1400	28.15	28.32	0.30	28.62	28.02	5				29.23	28.93									
7	2	0	N					313059	1400	28.15	28.32	0.20	28.52	28.02	6.5				29.49	29.19									
8	5	0	N	367	804	22819	1327								3	29.47				29.17	299.4	0.3	1	301.4	0.3	1	300.0	0.4	1
9	22	0	N	592	804	30086	1317								1.6	29.53				29.23	299.3	0.3	2	300.5	0.3	2	298.7	0.5	2
9	23	0	N	599	804	30249	1324								2	29.59				29.29	299.7	0.3	1	302.0	0.2	1	300.4	0.3	1
10	4	0	N					313059	1300	28.4	28.57	2.50	31.07	28.27	1	29.27	2	31.27		28.97									
10	5	0	N					313059	1325	28.3	28.47	2.50	30.97	28.17	1	29.1	2	31.1		28.8									
10	17	0	N					313055	1320	28.4	28.65	1.00	29.65	28.35	2.8	29.02	0.9	29.92		28.72									
10	18	0	N					313059	1320	28.5	28.67	1.00	29.67	28.37	2.8	28.91	0.9	29.81		28.61									
10	30	0	N	751	803	33658	1306								1.9	29.01				28.71	299.2	0.2	1	301.6	0.3	2	300.0	0.3	2
11	12	0	N					313059	1320	28.2	28.37	0.85	29.22	28.07	2.9	28.99	0.8	29.79		28.69									
11	13	0	N					313059	1325	28.3	28.47	1.60	30.07	28.17	2	29.25	1.3	30.55		28.95	301.6	0.4		304.9	0.2		301.1	0.2	
11	27	0	N	1076	803	100428	1304								6	29				28.7	299.7	0.2	0	301.8	0.2	0	299.0	0.5	1
11	28	0	N	1087	803	100468	1312								6	28.98				28.68	300.5	0.3	1	302.3	0.2	1	300.3	0.2	1
12	13	0	N	1146	803	100748	????	TIDBIT	110						5.4	29.32				29.02	294.0	0.7	2	299.8	0.2	1	297.6	0.2	2
12	28	0	N					313055	1320	28.6	28.85	0.80	29.65	28.55	3.2	29.21	0.7	29.91		28.91									
1	10	1	N					313055	1315	28.3	28.55	0.20	28.75	28.25	8	28.96	0.2	29.16		28.66									
1	11	1	N					376339	1320	28.3	28.30	0.50	28.80	28.00	3.8	28.85	0.5	29.35		28.55									
1	25	1	N	1335	802	101583	1251								8	28.36				28.06									
2	10	1	N	1411	801	101964	1214	313055	1300	27.8	28.04	1.00	29.04	27.74	3	28.11	0.7	28.81		27.81	303.3	0.4	1	299.6	0.2	1	299.8	0.4	2
2	11	1	N					313055	1220	27.8	28.04	0.90	28.94	27.74	3.2	28.21	0.7	28.91		27.91									
4	20	1	N					376339	1250	28.3	28.30	1.10	29.40	28.00	2.5		1	30.05	29.05	28.75									
4	21	1	N					376339	1250	28.3	28.30	0.80	29.10	28.00	3.3		0.7	29.55	28.85	28.55									
4	22	1	N					313055	1350	28.3	28.55	0.90	29.45	28.25	3		0.8	29.54	28.74	28.44									
5	29	1	N					342122	1250	29.2	29.21	2.10	31.31	28.91	1.5		1.7	31.19	29.49	29.19									
5	30	1	N					342122	1250	29.2	29.21	0.90	30.11	28.91	3		0.8	30.35	29.55	29.25	301.9	0.4		304.3	0.2		302.3	0.2	
5	31	1	N	1896	704	104415	1238	342122	1250	29.2	29.21	2.50	31.71	28.91	1		2	31.47	29.47	29.17	302.8	0.3	2	302.8	0.6	1	301.2	0.3	2

Table 2: Data used in the evaluation

Mo	DY	YR	D/N	SC1	SG1	Q-1	TB1c	VR1	All1	VR1c	SC2	SG2	Q-2	TB2c	VR2	All2	VR2c	SC3	SG3	Q-3	TB3c	VR3	All3	VR3c	SKNa	SKNb	VPcm
5	19	0	D	29.1	0.4	1						0.4	1					27.9	0.3	1							4.7
6	10	0	D																			0.00					5.5
7	2	0	D	28.1	1.0	1		2.44				0.9	1					29.3	0.2	0	29.48	0.16	29.48	0.04	29.68		3.7
7	3	0	D	31.1	0.4	1		2.75			28.6	0.4	1		0.83			29.5	0.2	1		0.00			29.48		3.6
7	25	0	D	30.4	0.2	0		0.04	30.17	0.037	27.8	0.3	0		5.61	30.17	5.61	28.6	0.2	1		2.41			30.17	30.17	4.8
8	5	0	D	30.7	0.4	2		0.40			25.5	0.4	2		21.34			28.0	0.3	1		4.41			30.07	30.07	5.0
8	29	0	D	28.8	0.4	2		3.45			27.1	0.4	2		12.94			27.6	0.3	2		9.59			30.69	30.69	4.1
8	30	0	D	31.7	0.3	0		1.04			28.6	0.3	0		4.66			29.5	0.2	1		1.46			30.71	30.71	3.3
9	22	0	D																						30.98	30.98	5.4
9	23	0	D	31.2	0.3	1		1.52			28.9	0.4	1		1.13			29.1	0.2	2		0.74			29.99	29.99	3.7
10	5	0	D																						29.46	30.55	4.7
10	6	0	D																						29.28	29.72	4.6
10	17	0	D																						29.46	29.11	5.6
10	18	0	D																						29.46	29.01	4.0
11	1	0	D	31.2	0.3	0		1.71	29.87	1.708		1.0	0					29.1	0.5	1		0.64			29.87	29.87	4.2
11	12	0	D																						29.18	29.19	3.6
11	13	0	D																						29.16	29.24	3.5
11	27	0	D	29.6	0.2	1		0.36			26.9	0.2	0		4.54	29.00	4.54	26.4	0.4	2		7.02			29.00	29	3.5
12	12	0	D	30.0	0.2	0		0.62	29.24	0.624	27.8	0.3	0		1.96	29.24	1.96	27.9	0.2	0		1.69	29.24	1.69	29.24	29.24	4.3
12	26	0	D		0.8	2						0.7	1					7.0	0.8	1					28.86	28.86	
12	28	0	D	29.6	0.1	1		0.01			27.3	0.3	1		4.98			27.1	0.2	2		5.72			29.50	28.91	5.0
1	11	1	D	29.8	0.1	1		0.34			28.0	0.2	0	29.20	1.47	29.20	1.47	28.0	0.1	2		1.42			29.20	28.85	3.6
1	27	1	D	28.7	0.1	0		0.11	28.41	0.114	27.0	0.3	0		1.88	28.41	1.88	27.1	0.2	1		1.74			28.41	28.41	4.4
2	11	1	D	25.6	0.1	1		9.97				0.4	2					25.5	0.6	1		10.82			28.81	28.21	3.7
2	12	1	D	22.7	0.1	2						0.3	1						0.5	2					28.40	28.15	4.8
2	27	1	D	27.3	0.4	1		5.38				0.5	1					25.4	0.6	2		17.64			29.57	29.57	4.6
2	28	1	D																						29.61	29.61	5.1
3	16	1	D	29.7	0.1	2		1.72			27.5	0.3	1		0.91			27.7	0.2	2		0.58			28.42	28.42	5.0
4	21	1	D																						29.00	29.05	5.3
4	22	1	D																						29.36	28.94	
4	23	1	D	30.8	0.1	0	29.11	2.94	29.11	2.931	28.3	0.2	1		0.69			28.7	0.2	0	29.11	0.20	29.11	0.20	29.11	28.84	5.4
5	11	1	D	29.7	0.2	0		1.40			27.6	0.2	0		11.38	29.93	5.6	28.2	0.2	1		7.71			30.93	30.93	6.0
5	12	1	D	29.2	0.2	0		0.04	29.43	0.038	26.7	0.2	1		7.25			27.7	0.2	1		3.04			29.43	29.43	5.8
5	30	1	D																						31.15	31.15	5.2
5	31	1	D	30.9	0.1	0		0.94	29.97	0.941	29.1	0.2	0		0.70	29.97	0.70	29.4	0.2	0		0.32	29.97	0.32	29.97	29.97	4.3
6	1	1	D	31.5	0.2	2		0.84			29.3	0.3	1		1.63			29.7	0.2	2		0.80			30.57	30.57	4.2
7	12	1	D	31.9	0.3	0	30.11	3.15	30.78	1.21	29.3	0.4	0	30.11	0.62			29.8	0.2	0	30.11	0.07	30.11	0.07	30.11	30.78	4.8
7	13	1	D																						30.71	30.18	5.3
8	3	1	D	27.9	0.7	1		8.31				0.4	2					25.6	0.2	1		26.41			30.77	30.88	5.7
8	4	1	D	27.9	0.1	2		5.74			25.7	0.4	1		21.10			25.8	0.2	2		20.63			30.32	30.32	5.8
8	26	1	D	30.8	0.1	0		1.83			29.3	0.2	0		0.04			29.0	0.2	2		0.19			29.48	29.48	3.8
8	27	1	D	31.5	0.1	1		0.29			30.3	0.2	1		0.37			29.9	0.2	1		1.18			30.95	30.95	
9	18	1	D	32.6	0.2	0		2.99	30.85	2.986	30.7	0.2	0		0.01	30.85	0.01	30.6	0.2	1		0.07			30.85	30.85	
9	19	1	D	31.4	0.1	0		0.32	30.86	0.323	29.9	0.3	0		0.93	30.86	0.93	29.7	0.2	1		1.38			30.86	30.86	
10	14	1	D	30.5	0.2	1		0.43			29.9	0.3	0		1.56			28.6	0.3	2		6.64			31.15	31.15	
10	15	1	D	32.6	0.2	0		1.82			30.4	0.4	1		0.80			30.5	0.2	1		0.68			31.28	31.28	
10	16	1	D	32.2	0.2	1		1.02			30.3	0.3	1		0.88			30.6	0.2	2		0.37			31.19	31.19	
7	1	0	N																						28.02		
7	2	0	N																						28.02		
8	5	0	N	28.2	0.3	1		0.93			26.9	0.4	1		5.27			26.3	0.3	1		8.38			29.17	29.17	4.9
9	22	0	N	27.3	0.3	2		3.64			25.6	0.5	2		13.29			26.1	0.3	2		9.78			29.23	29.23	4.1
9	23	0	N	28.8	0.2	1		0.23			27.2	0.3	1		4.38			26.5	0.3	1		7.58			29.29	29.29	3.0
10	4	0	N																						28.27	28.97	5.5
10	5	0	N																						28.17	28.8	4.6
10	17	0	N																						28.35	28.72	5.6
10	18	0	N																						28.37	28.61	4.8
10	30	0	N	28.4	0.3	2		0.09			26.8	0.3	2		3.64			26.0	0.2	1		7.11			28.71	28.71	3.4
11	12	0	N																						28.07	28.69	2.6
11	13	0	N	31.7	0.2	0	28.17	12.39			27.9	0.2	0	28.17	0.06	28.17	0.06	28.5	0.4	0	28.17	0.09	28.17	0.09	28.17	28.95	4.1
11	27	0	N	28.6	0.2	0		0.01	28.70	0.01	25.8	0.5	1		8.29			26.5	0.2	0		4.80	28.7	4.80	28.70	28.7	3.2
11	28	0	N	29.1	0.2	1		0.18			27.1	0.2	1		2.46			27.3	0.3	1		1.93			28.68	28.68	4.0
12	13	0	N	26.6	0.2	1		5.81				0.2	2						0.7	2					29.02	29.02	4.0
12	28	0	N																						28.55	28.91	5.7
1	10	1	N																						28.25	28.66	3.7
1	11	1	N																						28.00	28.55	3.8
1	25	1	N																						28.06	28.06	
2	10	1	N	26.5	0.2	1		1.58			26.6	0.4	2		1.20			30.1	0.4	1		5.52			27.74	27.81	3.7
2	11	1	N																						27.74	27.91	3.9
4	20	1	N																						28.00	28.75	5.6
4	21	1	N																						28.00	28.55	
4	22	1	N																						28.25	28.44	
5	29	1	N																						28.91	29.19	
5	30	1	N	31.2	0.2	0	28.91	5.08	28.91	5.062	29.2	0.2	0	28.91	0.06	28.91	0.06	28.7	0.4	0	28.91	0.03	28.91	0.03	28.91	29.25	
5	31	1	N	29.7	0.6	1		0.56			28.1	0.3	2		0.71			29.7	0.3	2		0.60			28.91	29.17	5.1

Table 2: (Continued)

Mo	month
DY	day
YR	year
D/N	day/night
SEQ	sequence
Proc	Processing Pipeline Version Number
IM#	Image Number
Tim	image time (GMT)
TB#	Tidbit serial #
TBtm	Time of tidbit data (GMT)
TBuc	Tidbit temperature, uncorrected
TBc	Tidbit temperature, corrected
DIUT	Temperature to be added to the tidbit temperature to equal an equivalent noontime value
DCT	Tidbit temperature, corrected with DIUT
SKN	Skin temperature for the corresponding tidbit temperature
TB#	Supplementary tidbit serial number
TBtm	Time of supplementary tidbit data (GMT)
TBuc	Tidbit temperature, uncorrected
TBc	Tidbit temperature, corrected
SP	wind speed, average for 6 hours prior to collection time
B0N	Buoy temperature, daily average at 1 meter depth at 0N, 165E.
DIUB	Temperature to be added to the buoy temperature to equal an equivalent noontime, near-surface value.
DCB	Buoy temperature, corrected with DIUB
B2N	Buoy temperature, daily average at 1 meter depth at 2N, 165E.
SKN	Skin temperature for the corresponding buoy temperature (0N or 2N)
GRD	Grad temperature
WSC	Western Most SCA
WSG	Std Dev. Western Most SCA
Q-W	Image Quality Western SCA
CSC	Central Most SCA
CSG	Std Dev. Central Most SCA
Q-C	Image Quality Central SCA
ESC	Eastern Most SCA
ESG	Std Dev. Eastern Most SCA
Q-E	Image Quality Eastern SCA
SC1	Mean temperature for SCA 1 area
SG1	Standard deviation of the temperature for SCA 1 area
Q-1	Image quality factor, 0= clear sky, 1= Cirrus, 2=clouds
TB1c	Tidbit data for clear sky only
VR1	Squared difference between SCA1 and tidbits(when available) or buoys.
All1	Tidbit or buoys for clear skies and diurnal buoy corrections less than 1C.
VR1c	Squared difference between SCA1 and tidbits(when available) or buoys, clear skies
SC2	Mean temperature for SCA 2 area
SG2	Standard deviation of the temperature for SCA 2 area
Q-2	Image quality factor, 0= clear sky, 1= Cirrus, 2=clouds
TB2c	Tidbit data for clear sky only
VR2	Squared difference between SCA2 and tidbits(when available) or buoys.
all2	Tidbit or buoys for clear skies and diurnal buoy corrections less than 1C.
VR2c	Squared difference between SCA2 and tidbits(when available) or buoys, clear skies
SC3	Mean temperature for SCA 3 area
SG3	Standard deviation of the temperature for SCA 3 area
Q-3	Image quality factor, 0= clear sky, 1= Cirrus, 2=clouds
TB3c	Tidbit data for clear sky only
VR3	Squared difference between SCA3 and tidbits(when available) or buoys.
All	Tidbit or buoys for clear skies and diurnal buoy corrections less than 1C.
VR3c	Squared difference between SCA1 and tidbits(when available) or buoys, clear skies
SKNs	Skin temperature of tidbits or buoys
SCNb	Skin temperature of buoys

Table 2. Column headings

5.1 Water Temperature Observations near the TWP-ARM Site at Nauru

The Atmospheric Radiation Monitoring (ARM) program was established by the Department of Energy to collect high quality meteorological data for Global Climate studies. The ARM monitoring site on the Tropical Western Pacific island of Nauru (Fig. 1), was selected to be an MTI validation site to take advantage of the wealth of meteorological and radiation measurements routinely collected and archived by the ARM project.

Figure 1. MTI image of Nauru.

Sea-surface temperatures are not routinely measured at the Nauru ARMSite. However, a cooperative agreement between the MTI and ARM programs directs the TWP climate observers to measure the water temperature at MTI image times.

5.1.a Instrumentation

The direct measurement of the water surface temperature is difficult and requires infrared radiometers because the surface skin layer is very thin (<<1mm) and is cooler than the deeper 'bulk' water. It is easier to accurately measure the deeper bulk water temperature but this temperature must be adjusted to account both for the cool skin and for any temperature gradient between the bulk water sensor and the near-surface temperature (warm-layer effect). The ground-truth water temperature measurements at Nauru were conducted as close to the surface as possible (10cm) so that the warm layer effect could be ignored. The cool skin problem is discussed in more detail in Section 5.2a.

A self-contained temperature data logger, called a TidBit, manufactured by Onset Computer Corporation was selected for the study because it is accurate, programmable, inexpensive, and easy to operate. TidBit programming and data downloading is accomplished with proprietary software and a personal computer.

Onset's specified accuracy for the Tidbits is 0.2C, with a resolution of 0.16C. The accuracy can be reduced to 0.1C with laboratory calibration but this accuracy is only realized as a mean of many data points. The response time of the Tidbit is ~3 minutes, which requires at least 10 minutes time in the water to converge to within 0.1C of the water temperature. At the Nauru site, data collection was initiated about 30 minutes before deployment, and continued for about 2 hours at a rate of 2 readings per sec.

5.1.b Calibration

Calibration of each TidBit was performed at SRTC prior to deployment with a stirred water bath. Figure 2 shows calibration data and the regression equation for the TidBit No. 313055. Typical RMS differences between the Tidbits and the water bath are 0.2C before correction and 0.1C after use of the regression equation, for the range 0-35C. To account for calibration changes with time and solar effects, we assume an absolute accuracy of 0.2C for the Tidbit data. The columns labeled Tbuc and TBc in Table 2 contain uncorrected and corrected Tidbit temperatures from Nauru at the GMT times given in column TIM.

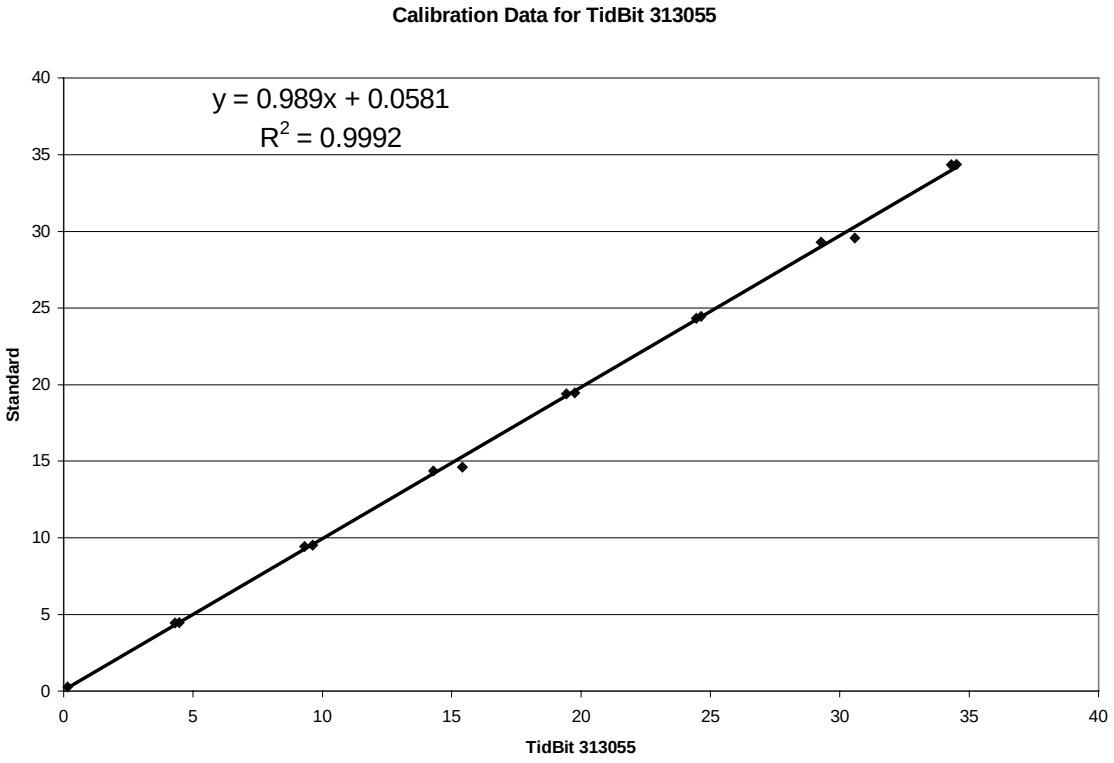

Figure 2: Calibration data for Tidbit S/N 313055

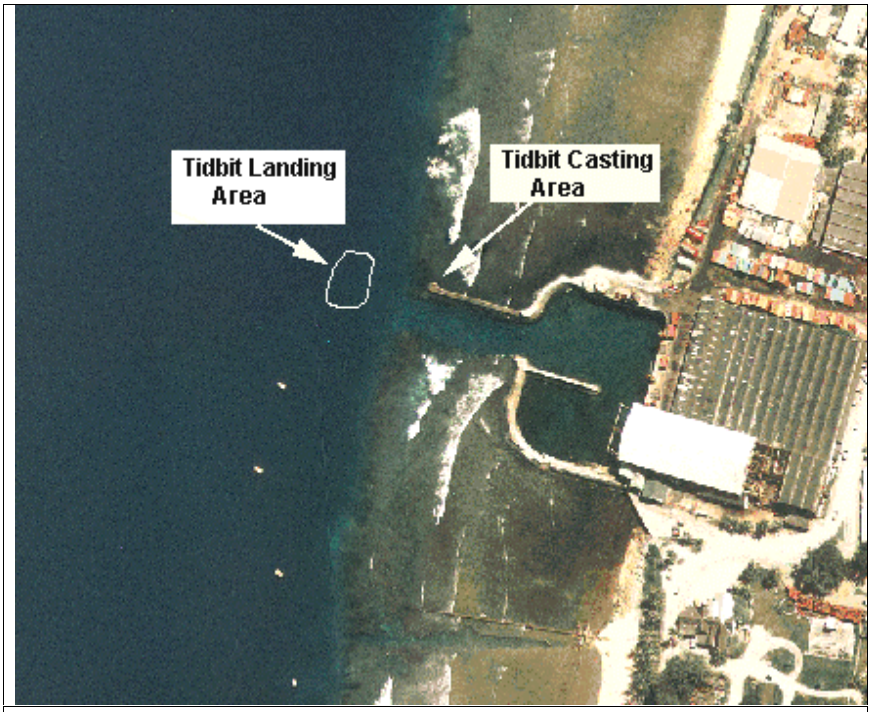

Figure 2. Photographs of TidBit Launching Sites near TWP-ARM

5.6c Tidit Deployment

The original TidBit launching apparatus consisted of a standard surfcasting rod with the TidBit suspended ~10 cm below a float (bobber). The Tidbit was cast into deep water from the seawall located about 1 km south of the TWP-ARM facility (Fig. 1 and Fig. 3). The seawall is the seaward boundary of a small boat harbor, and is about 3 m above the water level at high tide. (See Fig. 3).

After a site visit, SRTC personnel suggested the casting take place from the small jetty located 50 m northwest of the seawall. The jetty is about 0.5 m above water level at high tide, and extends further out to sea, which makes it possible to deploy the TidBit into deep water without its drifting back into shore. Due to safety concerns, the procedure was modified to cast from the jetty at low tide and at high tide only when sea conditions were calm.

Inspection of simultaneous water temperature observations made with the TidBit and NIST traceable standard (Omega Model XXXX) indicated a slight solar radiation effect due in part to the clarity of the water and the 10-cm depth of deployment. To reduce this effect the TidBit device was wrapped in aluminum foil.

5.1d Tidbit Data

Figure 4 shows TidBit data collected on 12/13/00 between 00:54 and 01:47 GMT. There were two casts on this day - the first at 01:05, was retrieved at 01:09 because the current brought the TidBit close to shore. (Note the rapid drop in temperature from 34C at 01:05 to about 29.5C at 01:09). A second cast at 01:09 was far enough so that the TidBit stayed away from the shore for about 20 minutes, and reached an average temperature of 29.4 C. The corrected temperature is 29.14 C using calibration equations shown in Fig. 2. Tidbit data are shown in Table 2, columns 9-12.

On several occasions a Tidbit was deployed from a Nauru Department of Fisheries boat ~50 m off-shore at the same time the temperature was measured with another Tidbit in the casting area to see if the temperature near the jetty is representative of the off-shore, deeper water. The TidBit deployed from the boat was cast into the water as the boat moved parallel to the shore about 50 m from the jetty. Figure 5 shows a daytime TidBit data on 02/12/01 between 00:40 and 01:50 GMT. Note that the boat tidbit temperature is ~0.2C warmer than that of the shore Tidbit.

Figure 6 shows nighttime Tidbit data from boat and shore on 10/04/00. In this case the boat temperature (S/N 313059) is 0.2C greater than the shore temperature. Figs. 5 and 6 suggest that the casting area is cooler than the open ocean. To further investigate this possibility, the temperature was measured from a boat that traveled from the tidbit casting location, and then out to 200 meters from shore with a precision, NIST-traceable recording thermometer suspended ~10cm below the surface. The boat track for two nightime collections is shown in Fig. 7 and the temperature data in Figs. 8 and 9. These figures show than for these two nights the casting area temperature was 0.2C and 0.3C cooler than 200 meters from shore.

Daytime temperature measurements from the boat (boat track in Fig. 10) are shown Figs. 11 and 12. On these days the casting area temperature was 0.1C cooler than off-shore on July 2, but 0.03C warmer on July 3, in contrast to the 0.2-0.3C cooler temperatures at night.

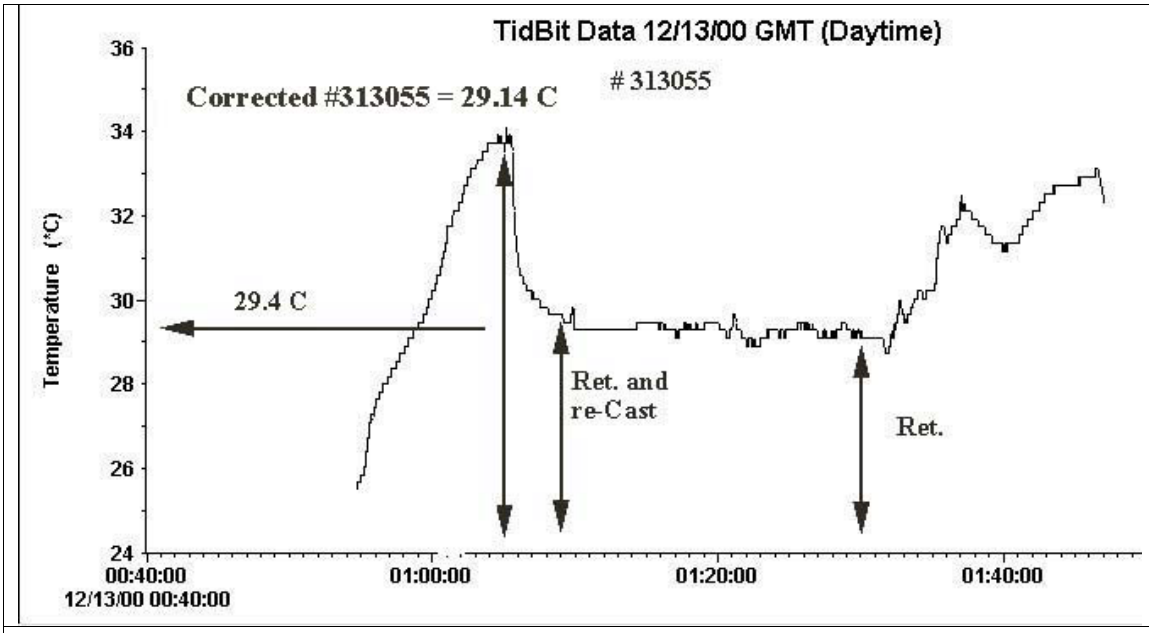

Figure 3. TidBit Temperature Data collected 12/13/00 near TWP-ARM.

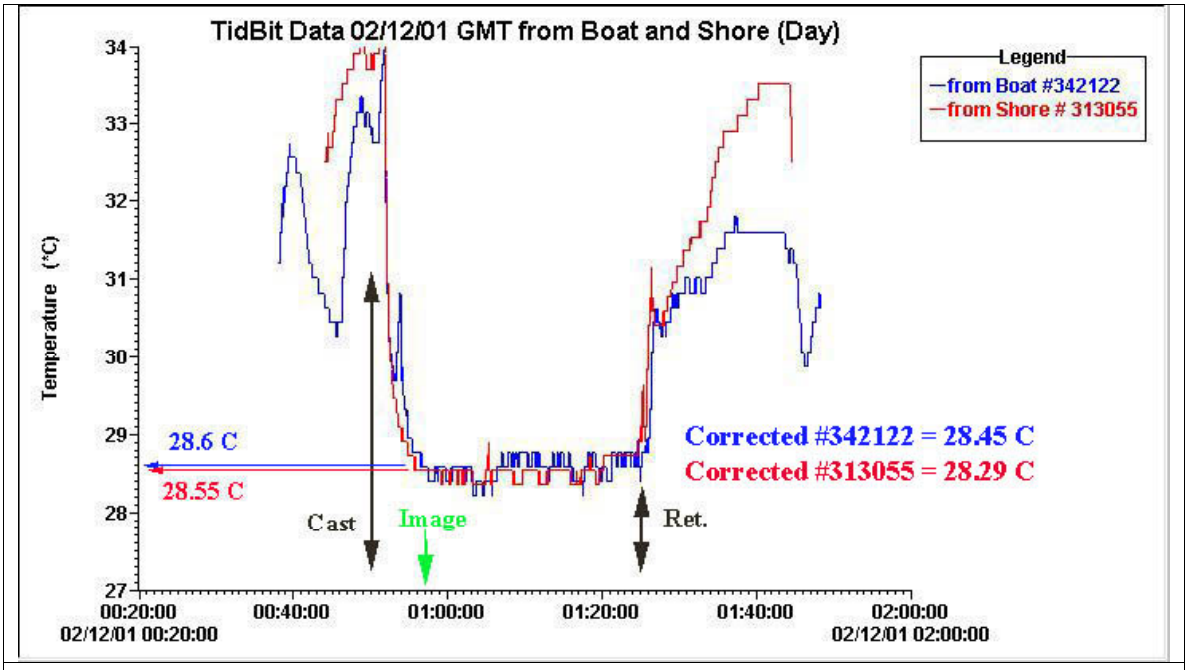

Figure 4. Comparison of TidBits deployed from Nauru Department of Fisheries Boat and the Shore on 02/12/01.

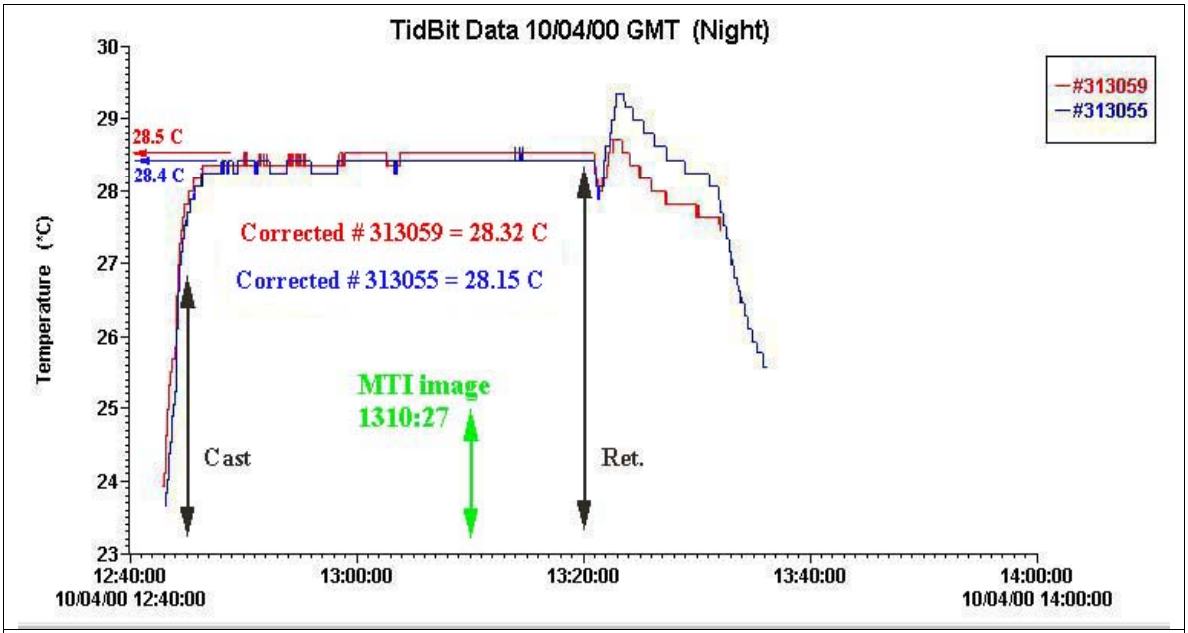

Figure 5. TidBit data deployed from Nauru Department of Fisheries Boat (S/N 313059) and the Shore on 10/04/00, night.

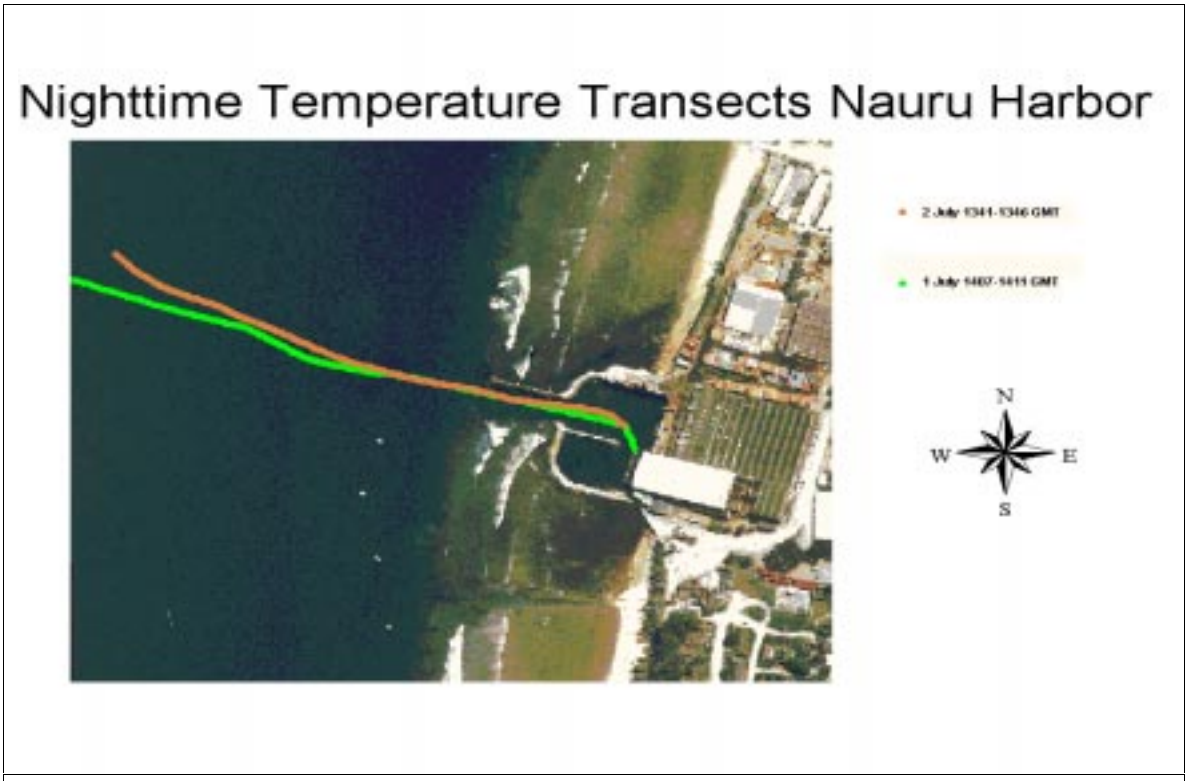

Figure 7. Nighttime track of the boat near the boat dock.

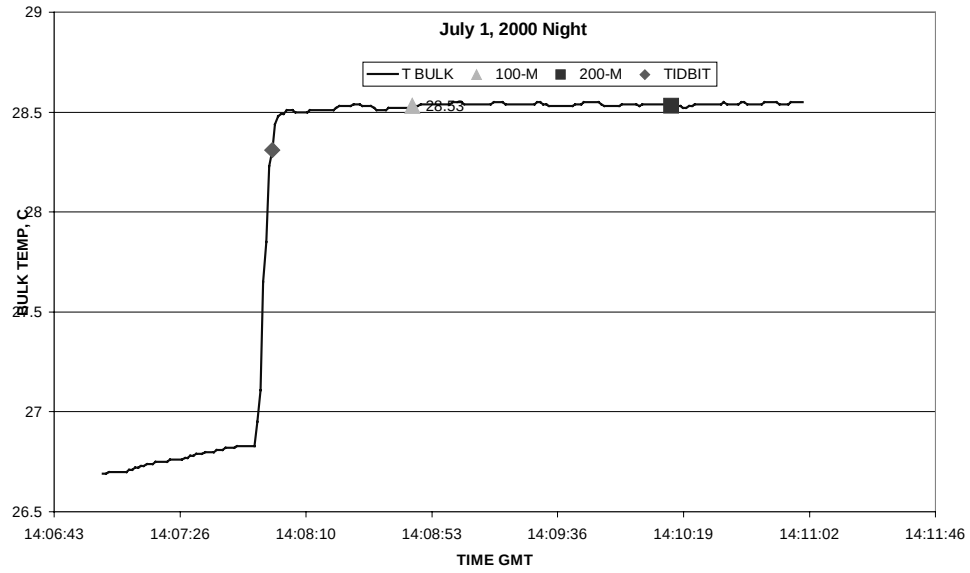

Figure 8. Nightime boat measurements on July 1, 2000.

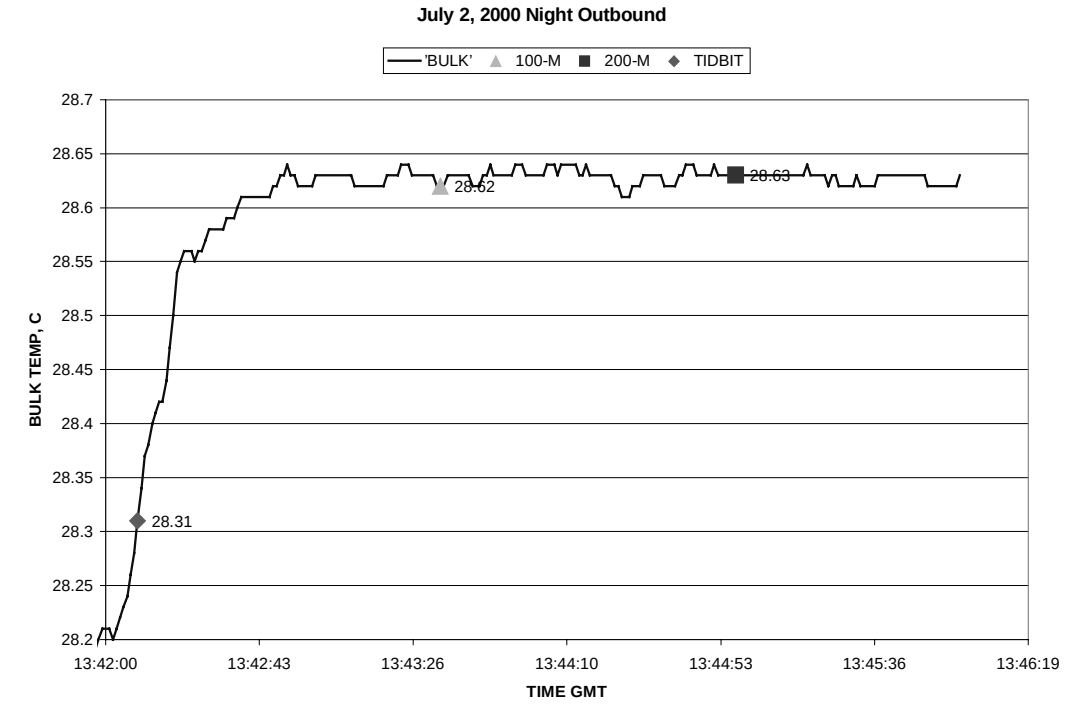

Figure 9. Nightime boat measurements on July 2, 2000.

The daytime boat mission also measured the surface water temperature with an 8-12 micron radiometer. Figs 11 and 12 show that the surface temperature is more variable than at a depth of 10cm temperature, and ~0.2C cooler at 100 meters than near the casting area (July 2).

The above results suggest a nighttime cold bias in the Tidbit casting area of 0.2C- 0.3C. This same bias was not as obvious in the daytime, possibly because the boat was only 100 meters from shore during the day.

Fairall et al. (2000) in a boat traverse around the island found that the bulk temperature (1 meter depth) was 0.1 – 0.2C cooler than upwind. However, their data were probably obtained further than 200 meters from shore.

In summary, Tidbit temperature data obtained from the casting area near the boat dock are probably cooler than temperatures in the open ocean by 0.1 to 0.3C. This difference may be due to the harbor or to an island wake.

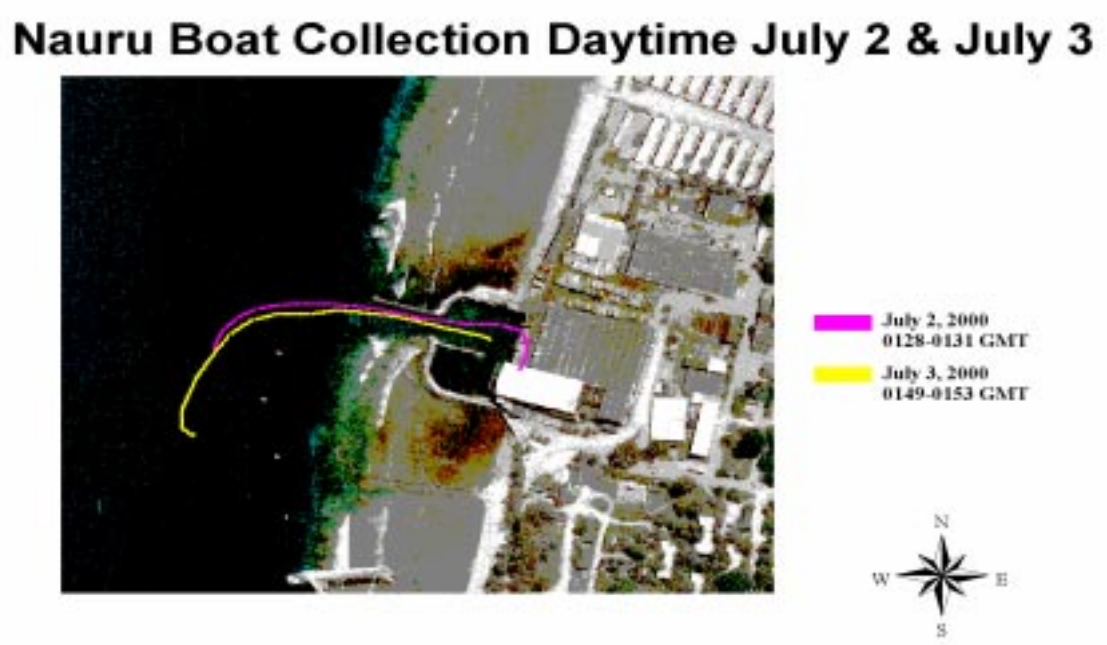

Fig. 10. Daytime boat tracks on July 2 1Fig. 10. Daytime boat tracks on July 2 and July 3, 2000.

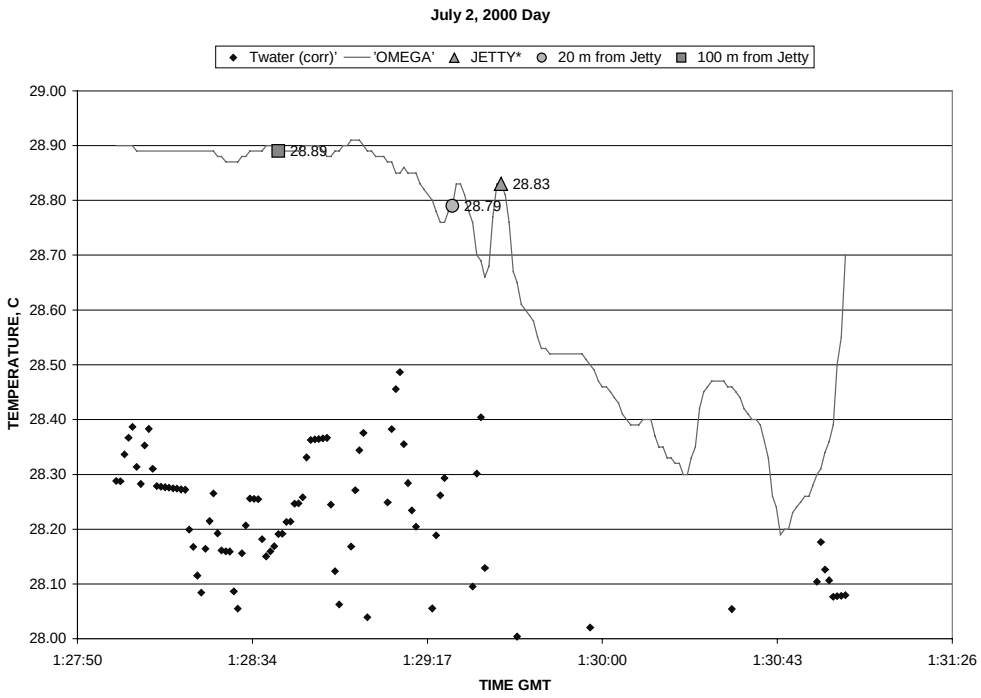

Figure 11. Boat measurements on July 2, 2000

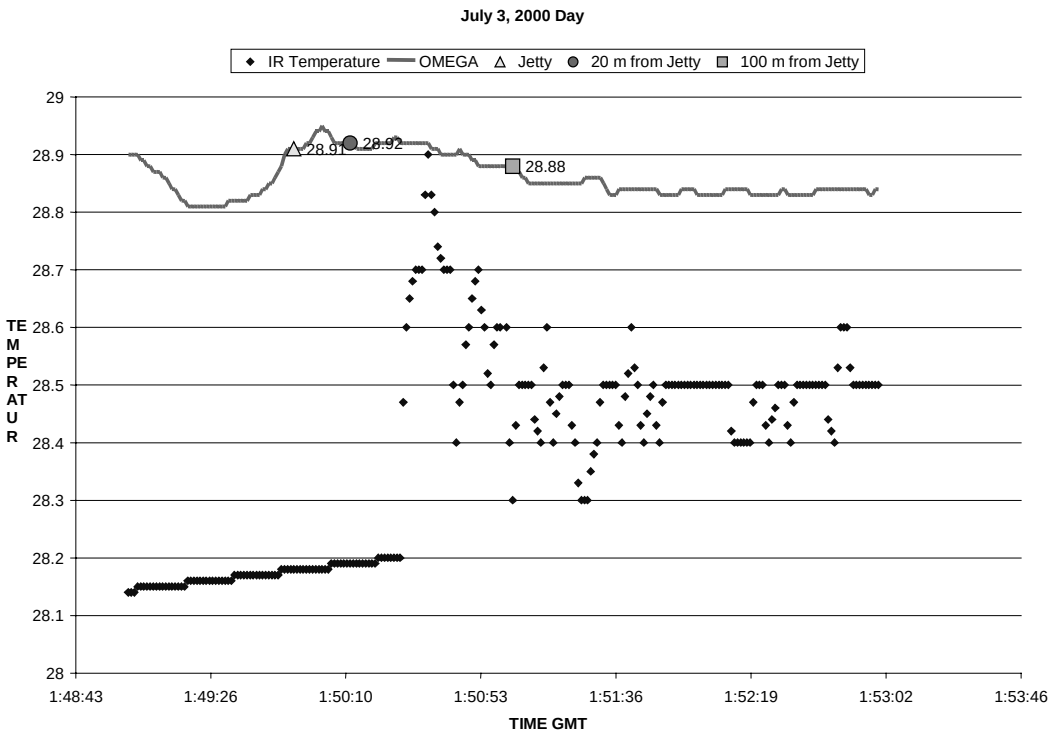

Figure 12. Boat measurements on July 3, 2000.

5.2 Buoy data

As noted in Section 5.0 buoy data are required to evaluate MTI-derived temperatures near Nauru because Tidbits were deployed during only 30% of the images. An added benefit of the buoy data, however, is that a comparison between the Tidbits and buoys is a valuable indicator of the accuracy of both data sets. In Section 5.2a we discuss the adjustments required to compare the two data sets, and also to calculate the sea surface temperature at the MTI image time.

The buoy data were obtained from the TAO/TRITON Tropical Atmosphere Ocean array of buoys (www.pmel.noaa.gov/tao.). In this network buoys are positioned every 2 degrees of latitude between 10S and 10N latitude at 165 East longitude. The buoys measure surface meteorological conditions as well as water temperatures at various depths with an accuracy of 0.02C. Data collected every 10 minutes are retrieved only during ship visits and therefore were not available for this comparison. On the other hand, daily averages are recovered by satellite in near real time and were used in this study[1]. The data from the buoy at 0N, 165E were used for this comparison when available. Otherwise, data from the buoys at 2N or 5S were used instead. (See columns B0N and B2N/5S in Table 2).

Gaps in the buoy data occurred during the MTI mission. Fig. 13, shows the bulk water temperature from the 165 East Longitude during the MTI period. An appreciation for spatial variability can be seen in Fig. 14, which shows buoy temperatures at 165 E, and 0, 2S, and 5S latitude for a two-month period. The RMS difference between the different buoys (~0.2C) is a measure of the error which occurs when buoy temperatures are used for locations ~200 km away. Difference in the surface temperatures may be even greater, however, because surface temperatures are more affected by wind, sky cover and rainfall.

5.2a Adjustments for the diurnal variation of temperatures

As mentioned in Section 5.0, in situ temperature measurements can be compared with satellite sea-surface temperatures only after making the warm layer and cool skin adjustments as described in Fairall et al. (1996). However, diurnal effects must also be considered when comparing 'instantaneous' measurements, e.g. Tidbits, or MTI retrievals, with mean daily buoy temperatures.

It is important to define several different temperatures before discussing diurnal effects. The *sea-surface* or '*skin*' temperature is measured by IR sensors and is the temperature of the top 0.1mm of the ocean. It is generally 0.1 to 0.5C cooler than the *near-surface temperature*, the temperature in the top few centimeters of the water. The *bulk water temperature* is the temperature usually measured from ocean ships, typically at a depth of ~1meter. The *deep water temperature* is the temperature at a depth of 20 meters or greater, i.e., deep enough to be unaffected by diurnal variations. The Tidbits measure the near-surface temperature and thus do not need correction for diurnal effects. The buoy depth is 1 meter and thus buoy temperatures must be adjusted to determine the corresponding near-surface temperature. Both Tidbit and buoy temperatures must be adjusted to find the corresponding skin temperature.

[1] 10-minute data are now (May 2002) available from the buoys near Nauru. However, since they exhibit little diurnal variation and are within ~0.1C of the diurnal average, they are not considered in this study.

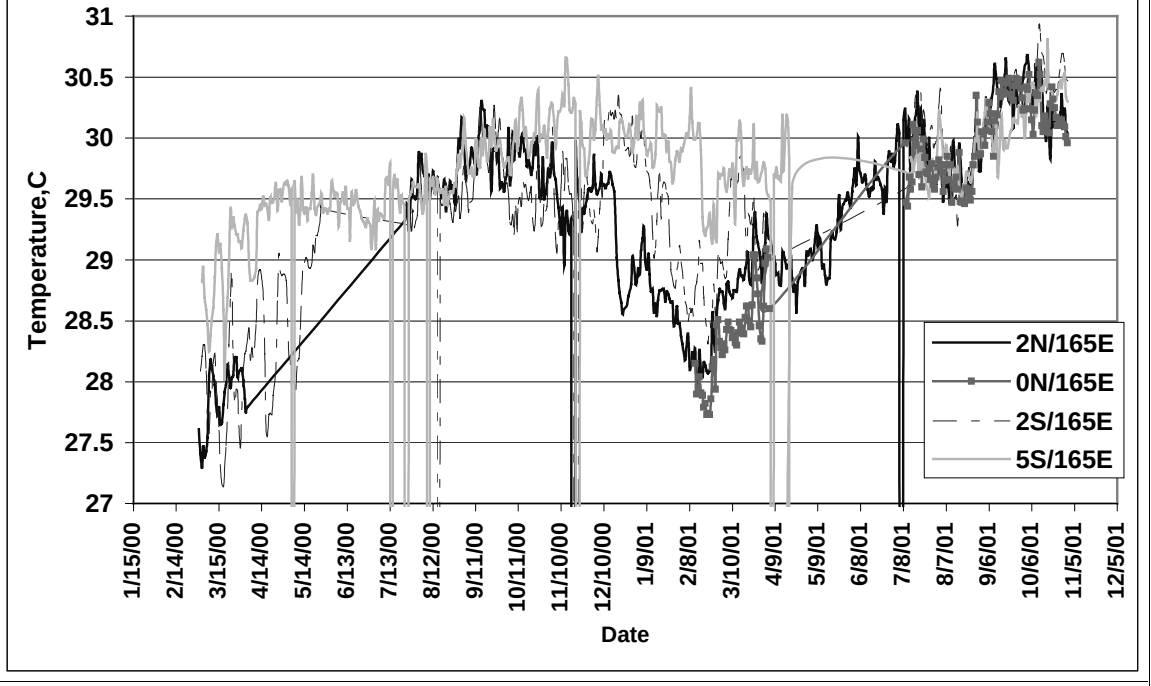

Figure 13: Buoy temperature (1 meter depth).

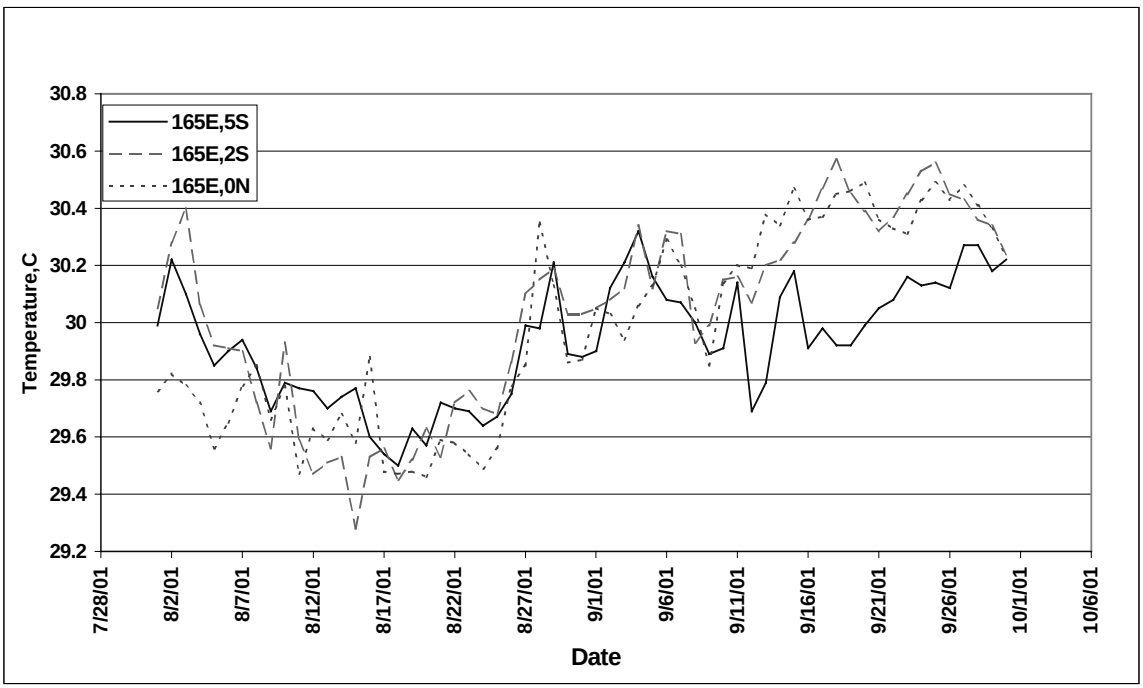

Figure 14: Buoy temperatures at 165E, July – Sept, 2001

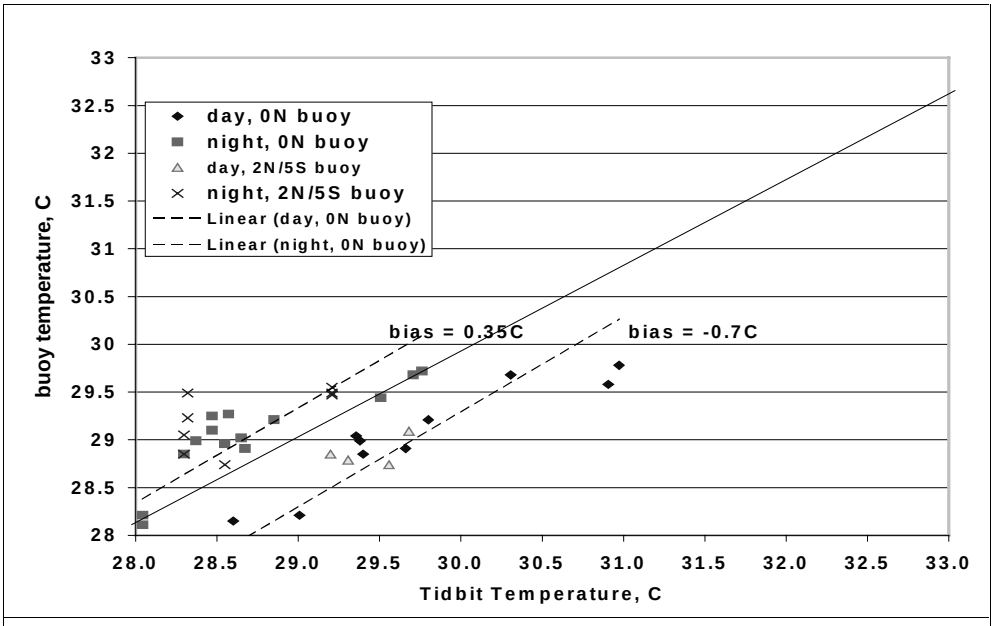

Figure 15. Comparions of the Tidbit and buoy temperatures

Figure 16. Warm layer temperature difference as a function of wind speed

A comparison of buoy and Tidbit data before diurnal effects are considered is shown in Fig. 15. The data were taken from Table 2 (columns TBC and B0N or B2N/5S). Buoy data from 165E and 0N were used when available and from 2N or 5S, otherwise. This figure reveals nighttime and daytime biases of +0.35C and –0.7C, respectively, of the buoy data with respect to Tidbit data. The daytime negative buoy bias is expected because the layer between 1 meter and the surface is warmed by solar heating. The nighttime positive buoy bias is also reasonable because the 1 meter mean daily value is more influenced by daytime heating than the midnight near-surface (Tidbits) value.

A buoy/Tidbit comparison requires that the buoy and Tidbit temperatures be converted to a common time and depth. This was accomplished with the results of Fairall et al (1996), who measured and modeled sea water temperatures in the Tropical Pacific Ocean.

As noted in Fairall et al (1996), the warm layer effect can be modeled in terms of a layer depth, D, and temperature difference ΔT between the near-surface temperature and the deep-water temperature, where diurnal effects are negligible.

To compare buoy data with tidbit data, we first use Fairall et al.'s Fig 8 to relate the warm layer temperature difference ΔT to the wind speed. This relation, given in Fig. 15**,** shows that the temperature difference is greater for light winds than for strong winds. Fairall et al.'s Fig. 8 can also be used to construct a relation between the warm layer difference (Fig. 16) and warm layer depth (Fig 17) as a function of wind speed and local time. Once the amplitude and depth of the temperature variation are known, the diurnal variation and daily mean at any depth can be found as a function of wind speed. (The average wind speed for the 6-hour period before each MTI image was obtained from the ARM surface observations and is given in column 'SP' of Table 2). Results are shown in Fig. 18. Finally, we can also calculate the difference between the near-surface temperature and that at any other depth as a function of local time. A summary of these results is shown in Fig. 19.

Figure 19 shows the adjustments required to convert local midnight Tidbit temperatures to corresponding noontime values (columns DIUT, DCT in Table 2), and daily mean temperatures at 1 meter depth to noontime values at 10cm (columns DIUB, DCB in Table 2). As the figure shows, the temperature adjustment is ~0.2C for strong winds and over 2 degrees for light winds. The light wind adjustment is greater because the solar heating is distributed over a much shallower layer.

The figure also shows the temperature increment which must be added to the midnight tidbit temperature to find the corresponding noontime 10-cm temperature. This difference is large because the near-surface temperature reaches a maximum near mid-day.

The adjusted buoy temperatures are plotted against the Tidbit data (daytime or adjusted nighttime) in Fig. 20. The day and night biases have been reduced to 0.1C and –0.15C, respectively, with an RMS difference of 0.42C. The RMS difference is important because it is an estimate of the uncertainty in the near-surface water temperature. Thus, the RMS difference between the MTI-derived temperature and the buoys /Tidbits is expected to be at least 0.42C, even if the MTI temperatures were without error.

As Fig. 20 shows, the nighttime and daytime bias of the buoys with respect to the Tidbits is positive and negative, respectively. The nighttime bias is more significant because at midnight the

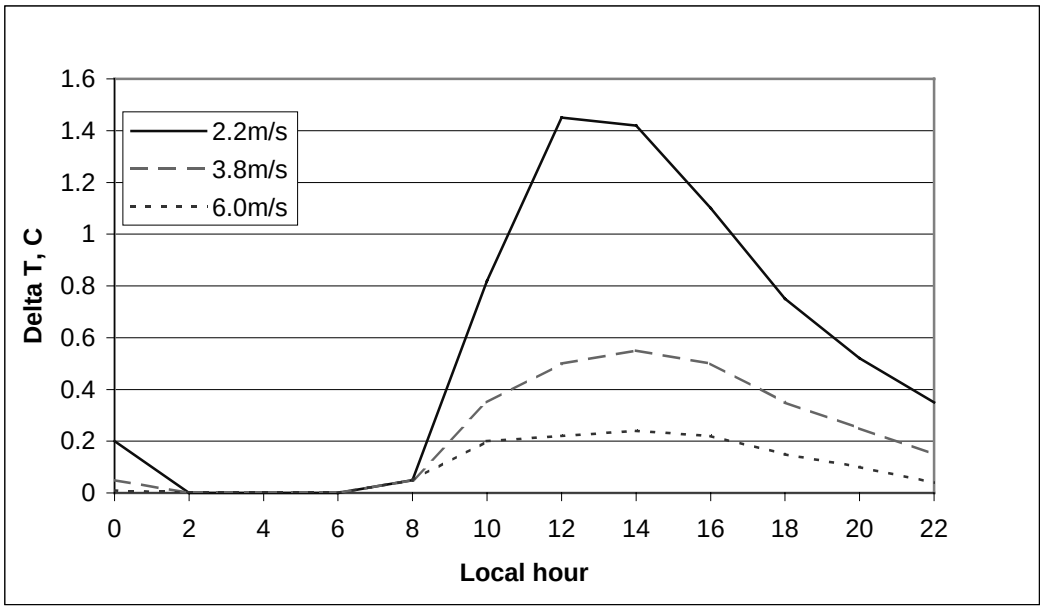

Figure 17: Warm layer temperature amplitude as a function of local hour

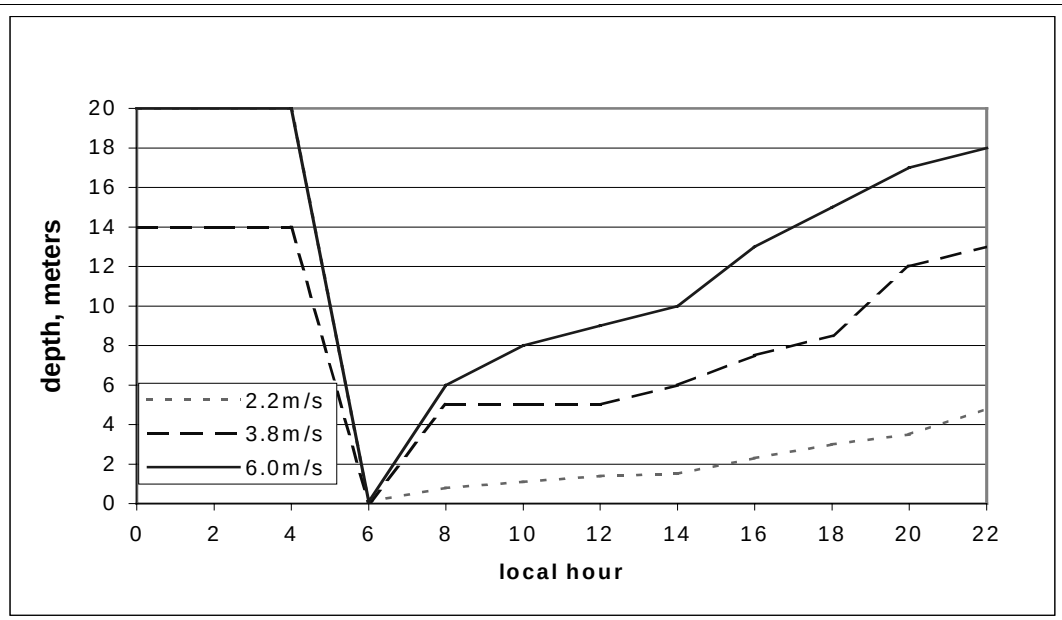

Figure 18: Warm layer depth as a function of the local hour

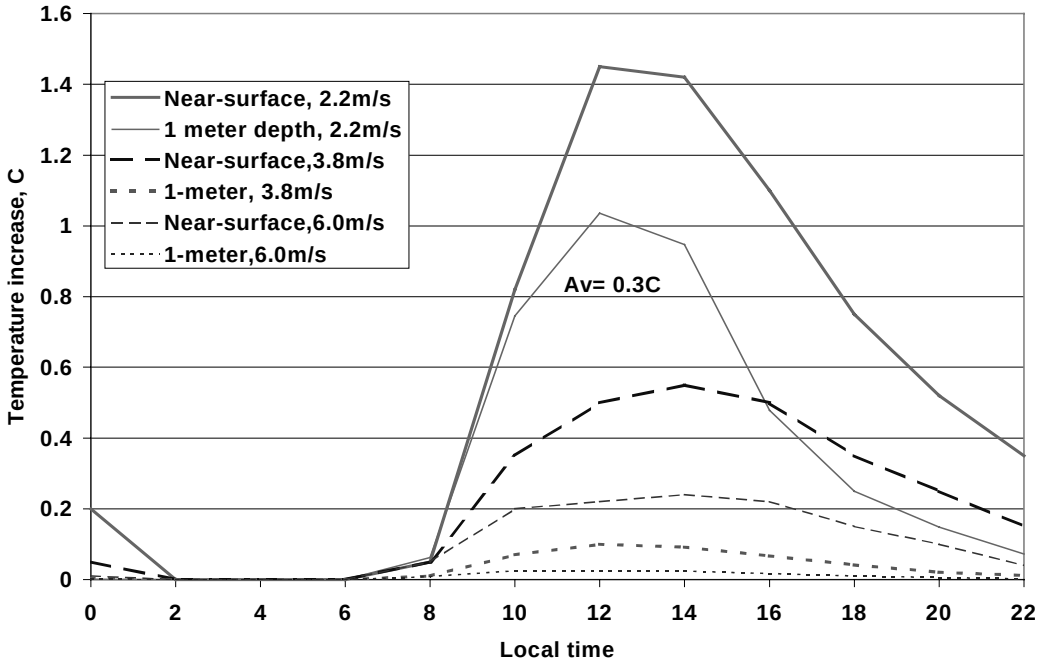

Figure 19. Delta T for near surface and 1 meter temperatures as a function of local time.

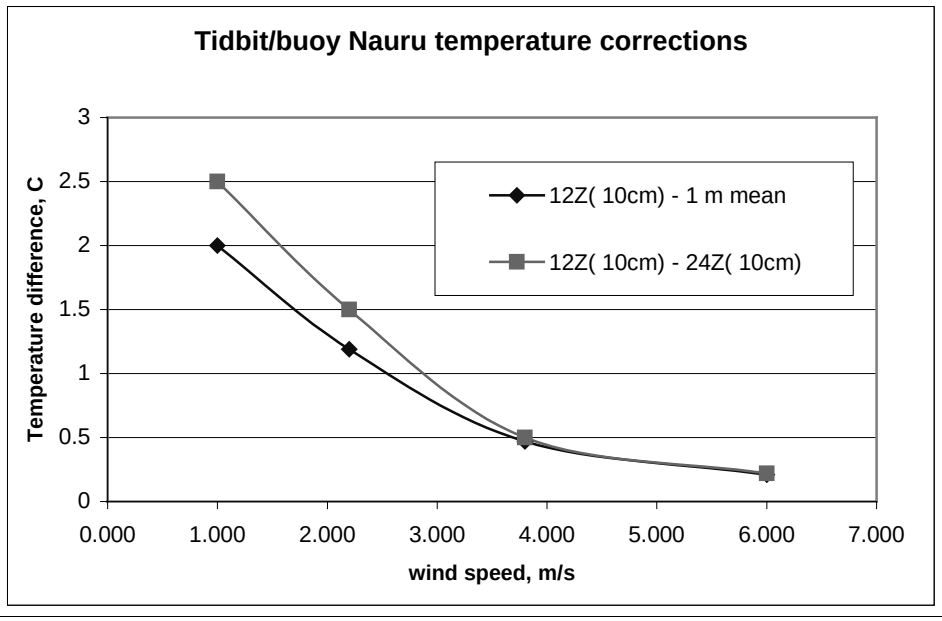

Figure 20. Temperature difference between noontime temperatures and midnight and 1 meter daily mean values.

near-surface temperature (Tidbit) should be very close to the buoy temperature, and little adjustment is required before comparison. In fact, the above analysis (Fig. 19) indicates that the midnight 10 cm temperature should be within 0.1C of its 1-meter mean daily value. However, as Fig. 22 shows, the nighttime Tidbit data is cooler than the mean 1 meter buoy data by ~0.4C. This difference may be due to spatial variability, as indicated in Fig. 1, but is more likely a manifestation of the cold harbor bias discussed in Section 5.1d.

In order to compare near surface bulk water temperatures with those inferred from satellite, it is first necessary to correct for the cool skin. This effect is a complicated function of heat exchange at the sea surface and ranges between 0.0 and –0.5C. In this paper we adopt the tropical Pacific results of Fairall et al. (1996), who found average skin depressions of 0.2 and 0.3C during the day and night, respectively. The skin temperatures for the tidbits and buoys are listed in the columns labeled 'SKN' in Table 2.

5.3 Uncertainty in the ground truth data.

Uncertainties in the sea-surface temperature derived from Tidbits or buoys are listed in Table 3. The sign and range is also listed in Table 3. The quoted values are for local noon and local midnight. The tropical Pacific ocean is relatively uniform over distances of ~10 km, and therefore we have assumed no variation in temperature over the MTI image, i.e., no uncertainty due to spatial variability for the Tidbits measurements. However, as noted in the last section, the near-shore Tidbits are probably biased low by 0.0C to -0.4C. An uncertainty of 0.2C is ascribed to spatial variability for the buoys (Section 5.2).

Warm layer and cool skin uncertainties are assumed to be 0.1C, except for daytime buoy temperatures, which have an uncertainty of ~ 0.5C.

The total uncertainty is simply the root of the summed variances and varies between 0.3 and 0.6C. This range is consistent with the RMS difference found for the corrected buoy and Tidbit data (0.42C, Fig 21).

Variable	**Tidbit**	**Buoys**	**Range**
Sensor accuracy	0.2	0.02	
Cool Skin	0.1	0.1	0.0 to -0.5
Warm layer (diurnal)	0.1	0.5(day), 0.1(night)	0.1 to +1.4
Island (harbor) effect	0.1(day), 0.2(night)	0	0.0 to -0.4
Spatial variability	0	0.2	0.0 to ±0.4
Total	0.3(day) 0.4(night)	0.6(day), 0.3(night)	

Table 3: Uncertainty (C) analysis of the sea-surface temperature derived from Tidbits and bouys.

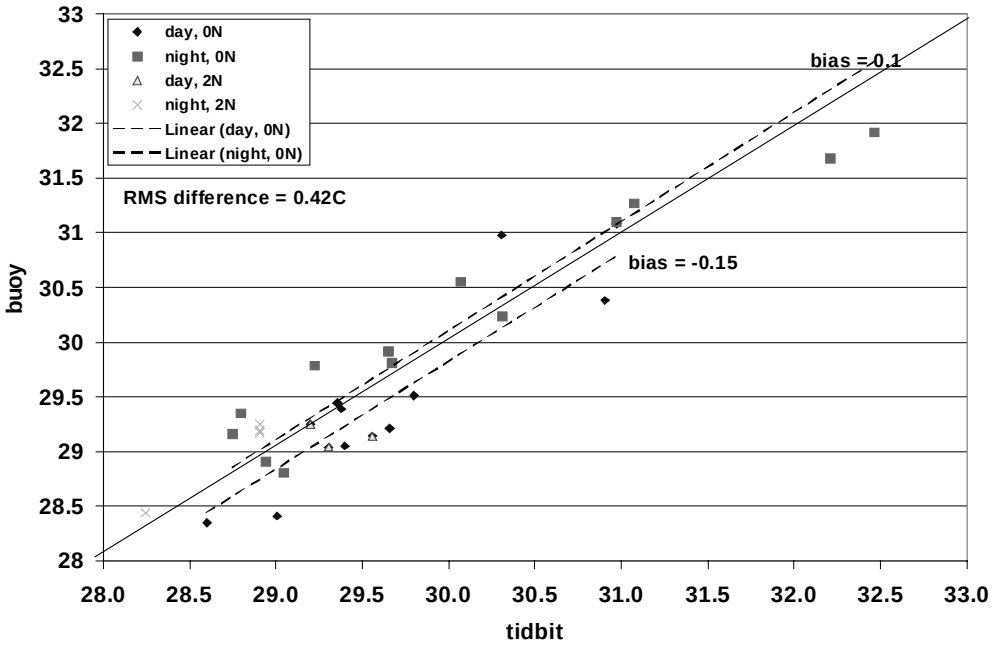

Figure 21. Near surface buoy and Tidbit temperatures, adjusted to local noon.

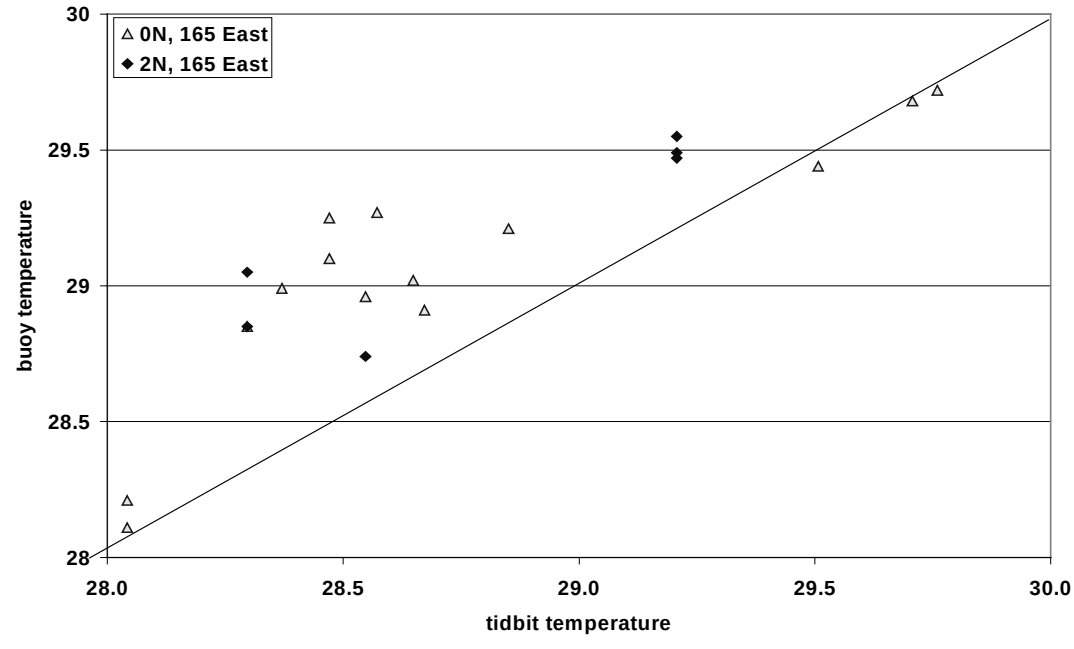

Figure 22: Midnight Tidbit and adjusted buoy temperatures

6. Analysis of MTI surface temperature data

Several factors influenced the selection of images to be used in the evaluation of MTI water surface temperature retrievals (WST). The most important factor was to compile a large enough database to make conclusions statistically significant, and next, to select images to cover at least one annual cycle. The initial selection produced a list of 55 images covering the period 5/19/00 to 9/27/01. The initial screening used rather "loose" selection criteria that required at least 50 % of the MTI image be cloud-free. As the study proceeded, images were divided into 3 quality categories based on the presence of clouds. To eliminate any bias in the results, this process did not utilize the ground truth data, but was based upon inspection of the WST image and "quick-look" images of the cirrus band (MTI band h). The following sections illustrate the procedure.

6.1 Subjective Assessment of Image Quality

Even though the SST in vicinity of Nauru is reasonably homogeneous, an examination of the WST from a typical MTI image revealed a wide range in temperatures over the image. See for example Figure 22 for MTI sequence number 485 collected 8/30/00 at 01:28 GMT (01:28 PM local). In this figure the most easily recognized features are the warm island (white) and the cold clouds (black). Also evident are the clear differences between the three Sensor Chip Assemblies, SCA's. For daytime images, the western, center and eastern sections of the image are SCA2, SCA1 and SCA3, respectively. At night the western and eastern sections of the image are reversed, i.e., SCA 3 and SCA 2 are west and east, respectively.

Figure 23 shows a WST bias between the SCA's with SCA1 significantly warmer than SCA3 which, in turn, is slightly warmer than SCA2. This bias is clearly evident in Figure 23, which shows the WST along three horizontal lines on 8/30/2000. The red curve corresponds to a cross-section along line 78, north of the island, the green curve is line 307, through the island, and the blue curve is line 632, south of the island. Notice within SCA1 and SCA3, the WST along line 632 is about 0.5C warmer than along line 78. No such variation is seen in SCA2.

Figure 24, shows a 3-band image for 8/30/00 with MTI bands h, g and the WST assigned red, green, and blue, respectively. The degree of "redness" is a measure of the amount of visible and sub-visible cirrus as radiance from band h is only significant when solar energy is reflected from high clouds, which are above most atmospheric water vapor. Cirrus along the northern portions of the image appears to reduce WST, which explains the apparent north-south gradient.

The above relationships were used as a means of categorizing various portions of the WST images in terms of a subjective quality factor ranging from 0 to 2. A quality factor of 0 denotes pixels unaffected by clouds and sub-visible cirrus. whereas a quality factor of 2 indicates a region strongly affected by clouds and sub-visible cirrus. Quality factors were determined independently for each SCA because of differences in the radiances and WST between the SCA's. The image quality is given in Table 2 for each SCA (columns Q-1, Q-2, Q-3).

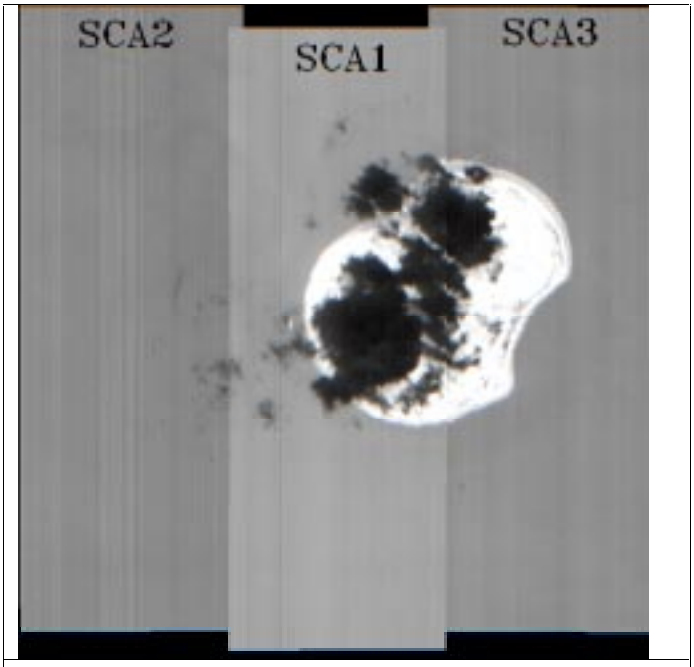

Figure 23. MTI image of wst temperatures for sequence 485, 8/30/00 0128 GMT.

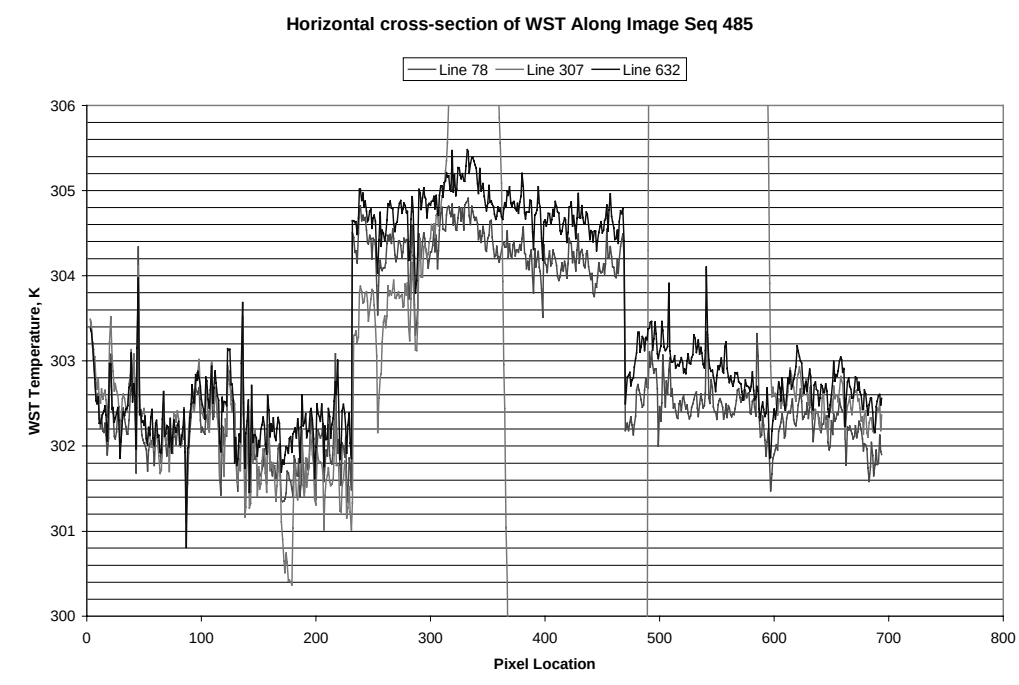

Figure 24. The WST along 3 east-west line on 8/30/00

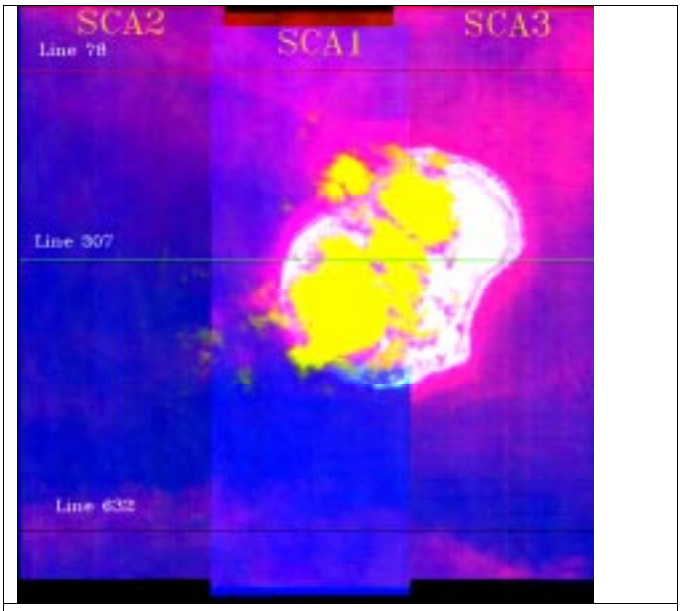

Figure 25. A 3-band image with bands h, g and WST assigned red, green, and blue, respectively on 8/30/00.

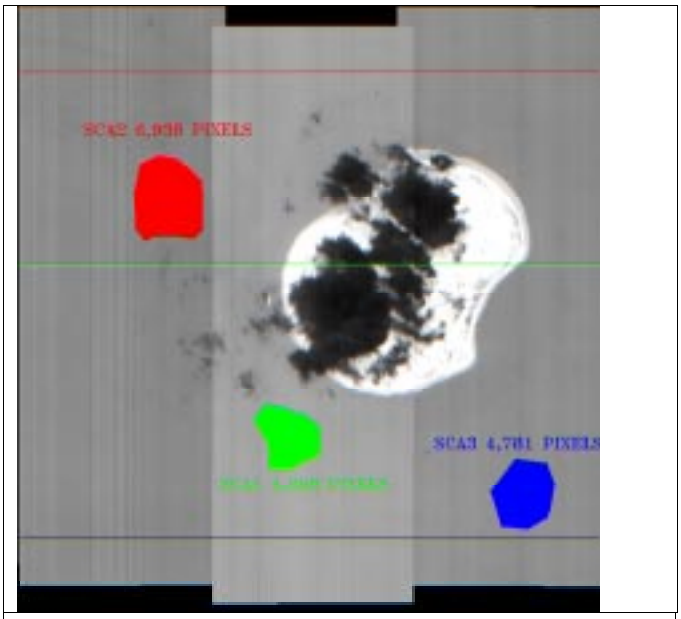

Figure 26. MTI WST image for 8/30/00 showing the three regions-of-interest for which temperature values were extracted.

6.2 Procedure for Selecting Representative SST Temperatures

Figure 25 shows the WST image with three irregularly shaped areas-of-interest within each SCA from which WST temperatures were extracted. The regions-of-interest were selected based upon an examination of the cirrus band image, the horizontal cross-sections and the wst image. Notice in this example the number of individual pixels within the regions-of-interest ranges from 4000 to 7000. Also note that had this been a nighttime image the selection of regions-of-interest would not benefit from the cirrus band and the regions would have not been so irregularly shaped. The quality factors associated with the western and central ROI was taken as 0 whereas that for the eastern ROI was 1.

Inspection of Figures 23 and 24 suggests that banding (anomalous pixel radiances) were not removed from the data before computing the brightness and surface water temperatures. Figure 23 also shows variation in surface temperature across the SCA's with a scale of ~ 1 km. This variation is apparent in all of the cross-sections shown in Fig. 24 and thus can not be due to clouds. The effect of pixel-banding is reduced by averaging across the ROI's, but the 1-km scale variations are comparable in size to the ROI's, and thus lead to additional uncertainty in the MTI water temperatures calculated in this study. Inspection of other Nauru images indicated generally less variability across each SCA's than seen in Fig. 24.

7. Results

As noted in Section 6, the MTI images can be separated into three groups, depending on the presence of cirrus or other clouds. The clear-sky retrieved temperatures are expected to be the most accurate. We also expect that the Tidbit data are more representative of the water around the island of Nauru than are the buoy measurements, despite the 0.1-0.4C cold bias in the Tidbit data. Therefore, we first compare the MTI surface temperatures with the Tidbit data for clear skies, when the temperature retrieval algorithm should be most accurate. MTI water temperatures and standard deviations are shown in Table 2 for each SCA (columns SC1, SC2, SC3, and SG1, SG2, and SG3). Tidbit clear-sky data are shown in column TB1c of Table 2.

Fig. 26 is a scatterplot of the three SCA's for this data subset. The bias of the MTI is shown and also the RMS difference between the MTI and the Tidbits. Although there are only 4-6 points for each SCA, some general conclusions can be drawn. The MTI derived temperatures for SCA 2 and 3 have biases and RMS errors of less than 0.6C. On the other hand, the MTI temperatures for SCA 1 are much worse, with a bias of +2.3C and an RMS of 2.5C.

The anomalous water temperatures derived from SCA 1 can be traced to the radiances in band L (8.0 – 8.4 microns). Fig. 27 shows radiances in bands K – N for the regions of interest on 8/30/00. Notable in these radiances is the 2% smaller radiance in the band L of SCA 1 compared to the other two SCA's. In band L, a 2% lower radiance corresponds to an ~1C cooler temperature. Note, however, that the robust algorithm (Table 1) multiplies the L band brightness temperature by –3.1, which implies that the lower radiances in band L of SCA 1 actually result in warmer calculated temperatures. This is why the WST temperature computed for SCA 1 is 2-3C warmer than for the other SCA's.

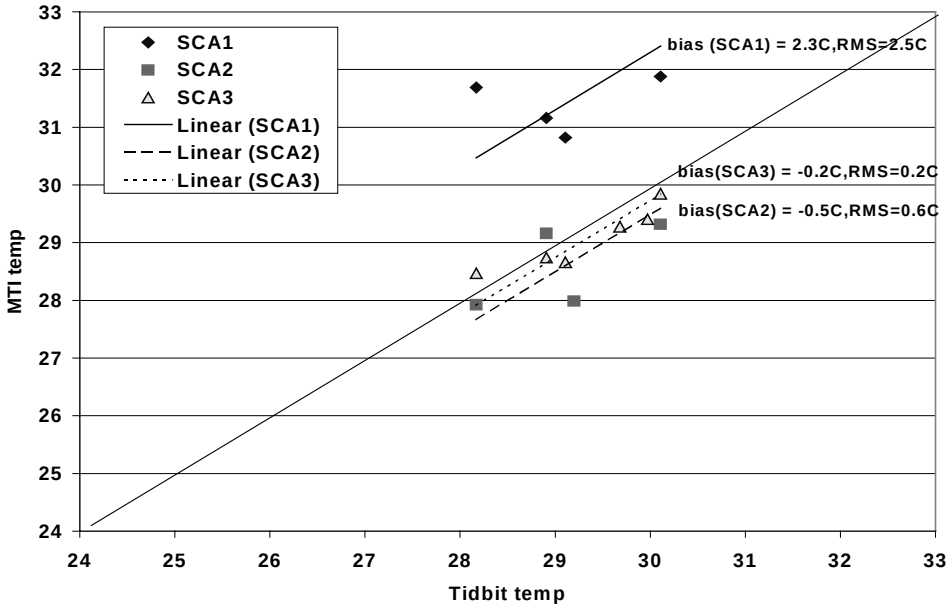

Figure 27. MTI vs Tidbits for clear skies

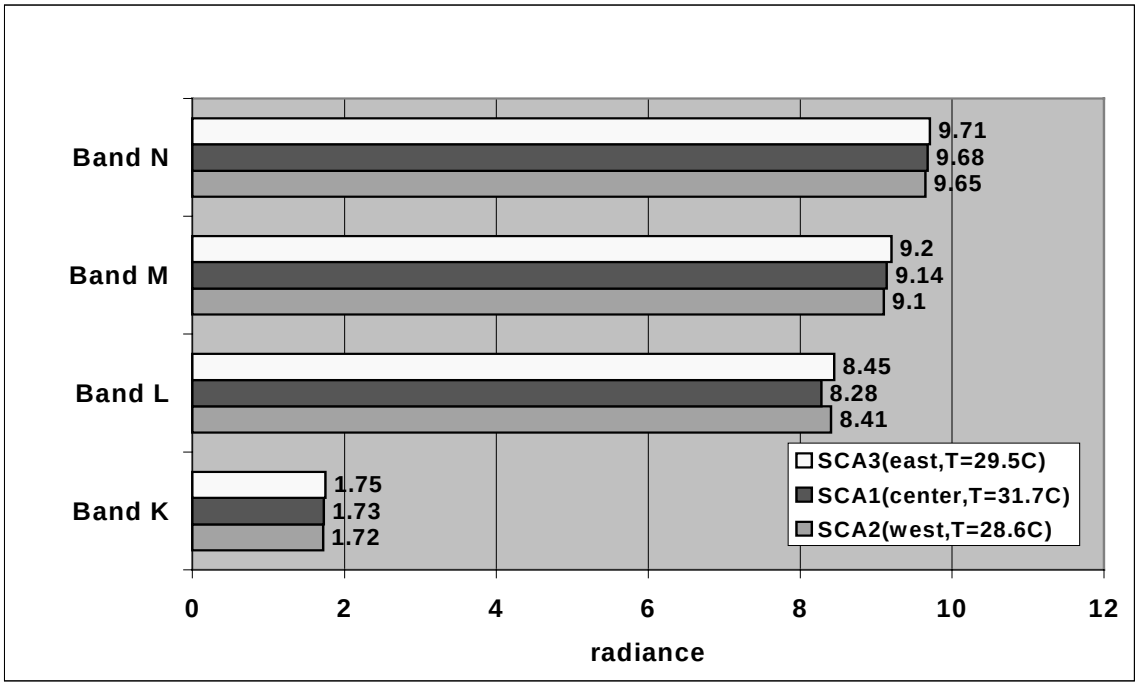

Figure 28. Radiance in Bands K,L,M and N for 8/30/00 (day)

Atkins et al, (2001) showed that the lower radiances in band L of SCA 1 are largely due to differences in the filter function rather than to radiometric calibration errors. This implies that these lower radiances are due to the wavelength-dependent atmospheric transmission, and the derived water temperatures will vary from scene to scene. Thus, a linear correction to the band L radiance may not improve retrievals at all locations.

The RMS error obtained for SCA's 2 and 3 under the optimum conditions shown in Fig. 27 is consistent with the design specifications of the MTI. The quoted radiometer accuracy in the IR bands is 1%, which corresponds to a brightness temperature accuracy of 0.8% for a 350C target (no atmosphere) and an uncertainty due to atmospheric variability of 0.8% [2]. The use of 4 IR bands should improve the accuracy of derived temperature somewhat, but 1% remains the best estimate of the expected accuracy under optimum conditions.

We must also keep in mind the 0.42C RMS difference between the buoys and Tidbits discussed in Section 5.3. This implies that part of the variance shown in Fig. 26 is from errors in the ground truth sea-surface temperatures instead of the MTI results.

The relatively few cases shown in Fig. 27 can be increased if we include the buoy temperatures, but again consider only clear sky (optimum) conditions. Results for the 3 SCA's are shown in Figs. 29, 30, and 31. This comparison only considers cases when the warm layer correction was less than 1C, i.e., brisk winds. As can be seen from these figures, the addition of the buoy data has improved the agreement for SCA 1 but made it worse for SCA's 2 and 3. The RMS difference now ranges between 0.94 and 1.5C. The increase in RMS errors is partly due to the cold bias of the Tidbits with respect to the buoys, discussed in Section 5.2.

A comparison of MTI retrievals with all ground truth data is shown in Figs. 32-34. These figures show that when all data are included, the variance increases and the MTI temperatures become more negatively biased (cooler) with respect to the ground truth. This trend is understandable since the presence of any clouds in an image will tend to lower the inferred sea-surface temperature.

Since the robust method is a regression over many different atmospheric cases, it is likely that the accuracy of the surface water retrieval will be worse for extremes in the atmospheric water vapor and temperature. To examine the dependence on water vapor, Fig. 35 shows the error in the SCA1 retrievals as a function of the column water amount. The water vapor column was obtained from the microwave water radiometer at the Nauru ARM site at image time. This figure shows that the data can be divided into a main group, with errors between –0.5 and 2C, and outliers with errors of –1.0 to –5.5C. A subset of these outliers has precipitable water near 6 cm while a second subset includes the range between 3.5 and 5 cm. The main group of data, however, shows no dependence on precipitable water. This suggests that the outliers are not the result of extremes in water vapor.

Because of hardware problems that occurred during the MTI mission, the accuracy of retrieved water temperatures may have worsened during the mission lifetime. Fig. 36 shows nighttime WST temperatures from July, 2000 to Ocober, 2001 vs. buoy temperatures. This figure shows no significant degradation in retrieved accuracy over this 15-month period. If anything, the variance is actually less in the last 5 months than in the first 5 months, i.e., the retrieved water temperature became more accurate with time.

[2] S. Bender, LANL. Personal communication, May 2002

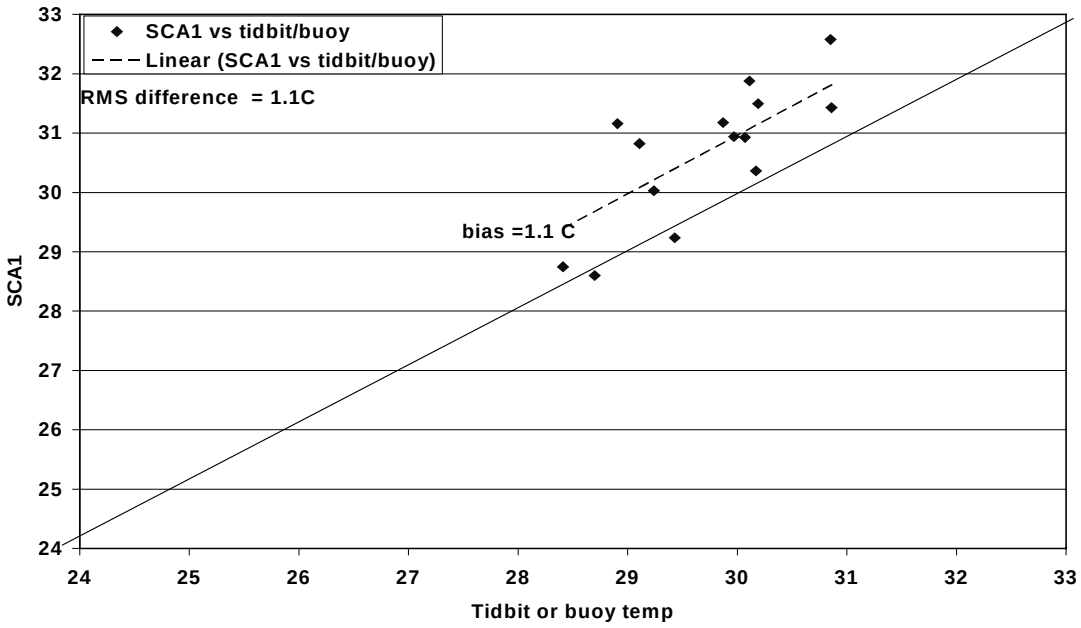

Figure 29. SCA1 vs Tidbit/buoys for clear skies withthe diurnal correction less than 1C

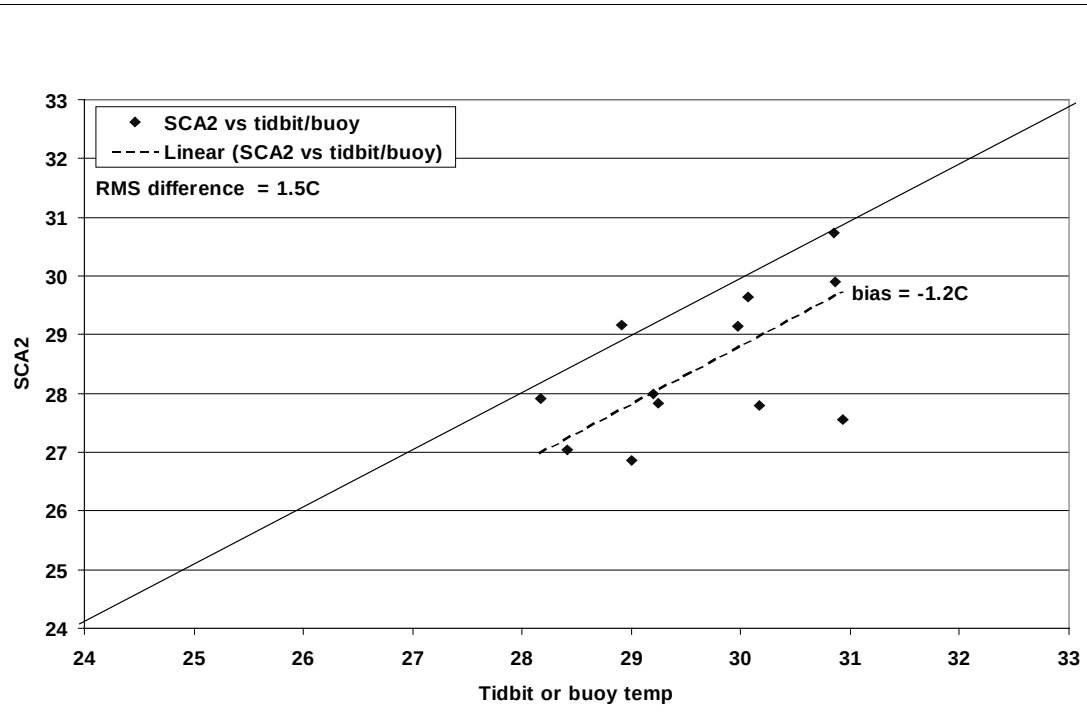

Figure 30. SCA2 vs Tidbit/buoys for clear skies with diurnal correction less than1C

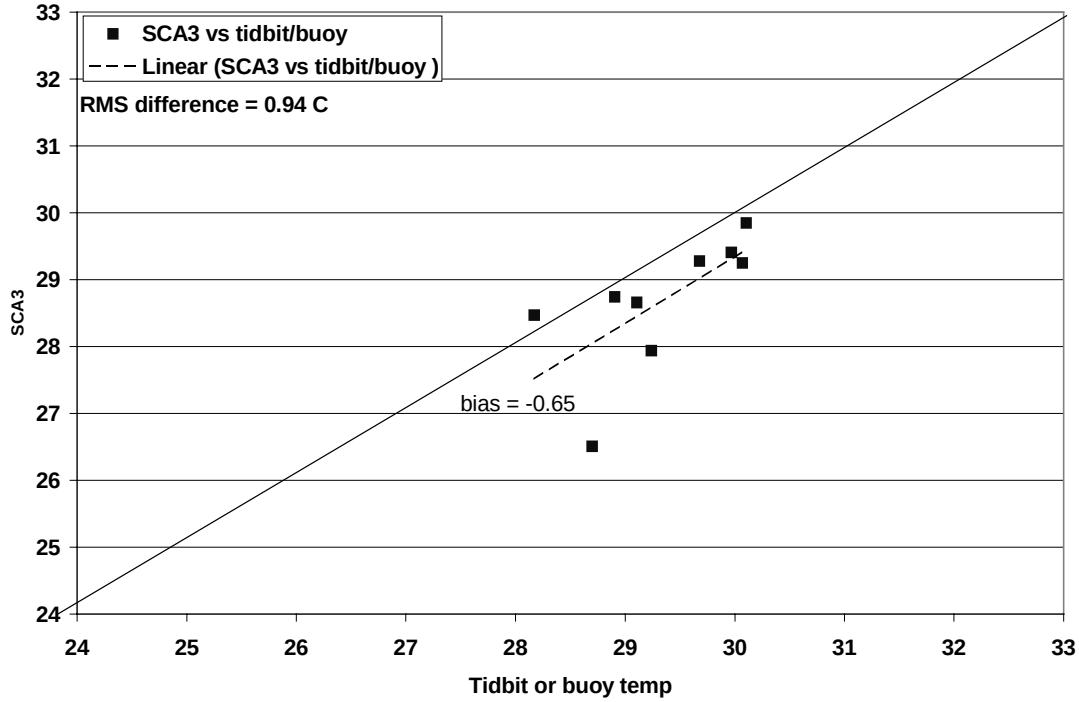

Figure 31. SCA3 vs Tidbit/buoys for clear skies with diurnal correction less than1C

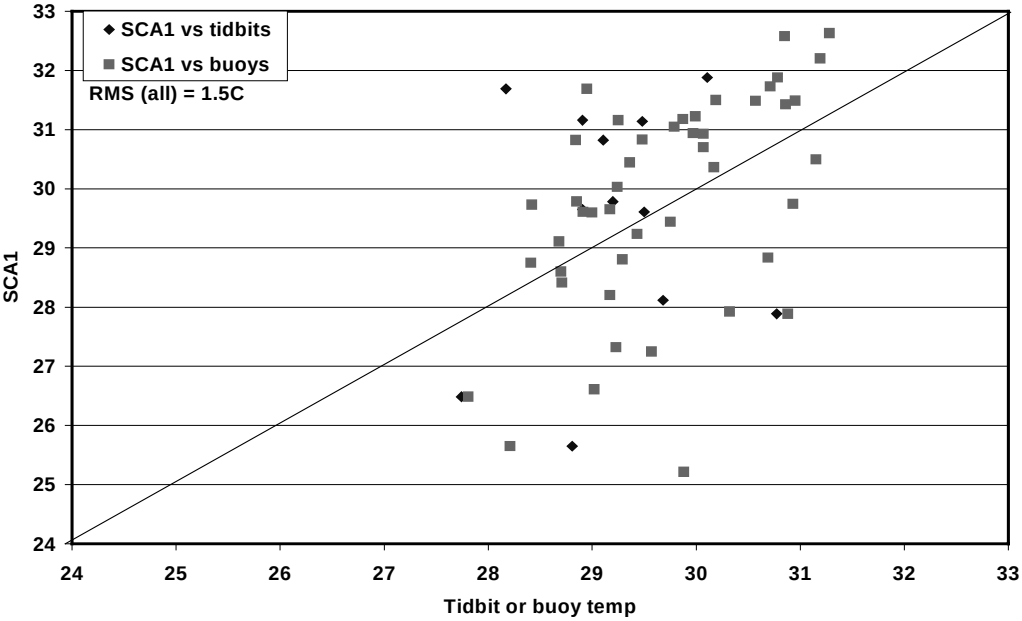

Figure 32. SCA1 temperatures vs all Tidbits/buoys

8. Conclusions

The RMS error of Tropical Western Pacific Ocean surface water temperature calculated with the robust retrieval algorithm is ~1C for ideal, i.e., clear sky, conditions. This RMS error includes likely biases of ~0.5-1.5C in the three SCA's. These biases are probably the result of differences in the wavelength dependence of the transmission filter of the SCA's rather than to radiometric differences. Thus, the brightness temperature (and calculated water temperatures) SCA difference will vary from scene to scene.

The RMS error also includes errors in the ground truth sea-surface temperature, which are estimated to be ~0.4C. Thus, the actual error in the MTI retrievals for ideal conditions is probably less than 1C, i.e., on the order of –0.7C.

When partially cloudy images are included, the RMS error of the robust retrievals increases to ~2C. These partly cloudy conditions almost always add a cold bias to the retrievals because cloud temperatures are invariably cooler than the underlying water temperature.

The retrieval error was not dependent on the water vapor column amount, nor did it change significantly during the 15 months of this study. If anything, the retrieval error was less at the end of the mission than at the beginning.

The results suggest that the accuracy of the retrievals for clear sky conditions could be improved to ~0.5C if radiances are preprocessed to remove anomalous pixels and the above mentioned biases. Before this is attempted, however, it is necessary to determine the performance of the robust method for cold target sand varying atmospheric conditions. Errors for scenes with clouds retrieval can only be improved by correcting for the presence of clouds.

9. Acknowledgements

We are grateful to Bill Clodius of Los Alamos National Laboratory for providing valuable information on the LANL robust method and to Kim Pollack and Kim Starkovich of LANL for processing the MTI images used in this study. We thank Steve Bender and Bill Clodius of LANL for critical reviews of the manuscript.

10. References

Atkins, W., S. Bender, W. Christensen, C. Little E. Riddle, 2001. The Multispectral Thermal Imager Calibration. Presented at the *MultiSpectral Thermal Imager Symposium*, Sandia National Laboratory, March 12-13, 2001.

Fairall, C. W., E.F. Bradley, J.S. Godfrey, G. A. Wick, J.B. Edson, and G. S. Young, 1996. Cool-skin and warm-layer effects on sea surface temperature. *J. Geophys. Res*, 101, 1295-1308.

Fairall, C. W., M.J. Post, J.E. Hare, A.B. White, and A.A. Grachev,2000. Preliminary examination of island effects on near-surface bulk meteorology and air-sea fluxes from the Nauru99 field program. *Proceedings of the Tenth ARM Science Team Meeting*, San Antonio, Texas, March 13-17, 2000.

Tornow,C. and C. C. Borel, 1994. Multi-angular multi-spectral night-time water temperature retrieval. *MTI Technical Report MTI-94-001*.

Tornow, C. C.C. Borel, and B. J. Powers, 1994. Robust water temperature retrieval using multi-spectral and multi angular IR measuremnets, *Proc. IGARSS '94*, 441-443, 1994.

11 Appendix

Extensive data sets were used in preparation of this report. This data has been collected on a CD-ROM for possible future use. The disk entitled, 'Comparison of MTI and Ground Truth Sea Surface Temperatures at Nauru: Appendix', contains supplementary files generated while processing the MTI images and also data files from the DOE ARM site on the island of Nauru on MTI image days. The image files are stored in directories named for each MTI sequence number in Table 2. These directories contain TIF images with the selected regions of interest identified (see Section 6) and statistical summary files for each area of interest, including number of pixels, and the mean, minimum, and maximum temperature plus the standard deviation. Files of the temperature across northern, central, and southern lines of the image (e.g. Figure 24) are also included.

The Appendix also contains Nauru ARM data. This data is in cdf format and includes microwave water radiometer profiles, surface meteorology, and radiosonde soundings. Each file name contains the year, month, day and GMT time of the data. Three examples are given below. Note that data for some time periods was not available.

wpmwrlosC2.b1.20010211.000012.cdf	microwave water radiometer
twpsmet60sC1.b2.20010917.000001.cdf	surface meteorology
twpsondewnpnC2.a1.20000518.234400.cdf	radiosonde

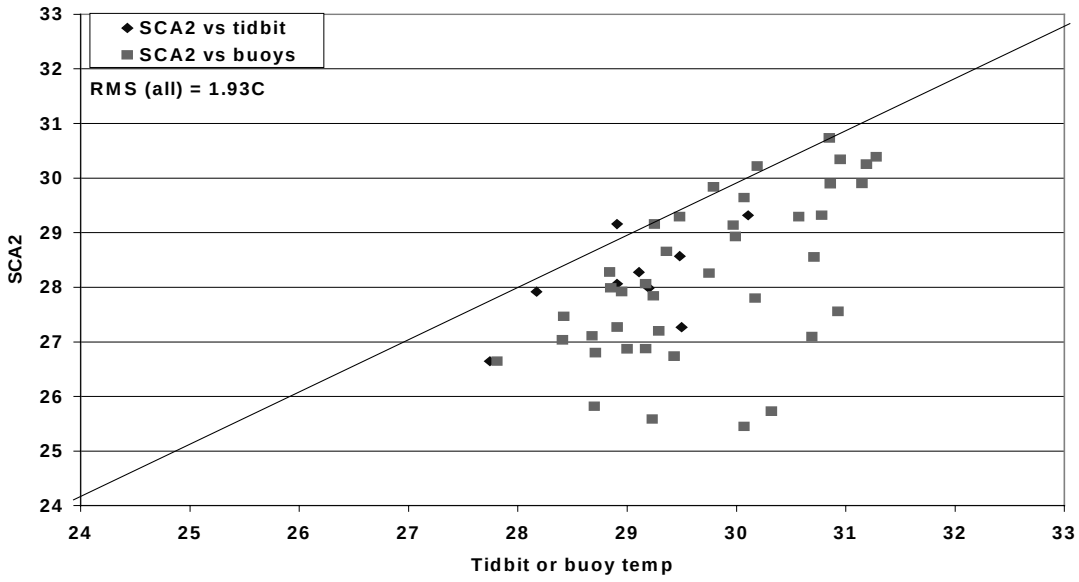

Figure 33. SCA2 WST temperatures vs all Tidbit./buoys

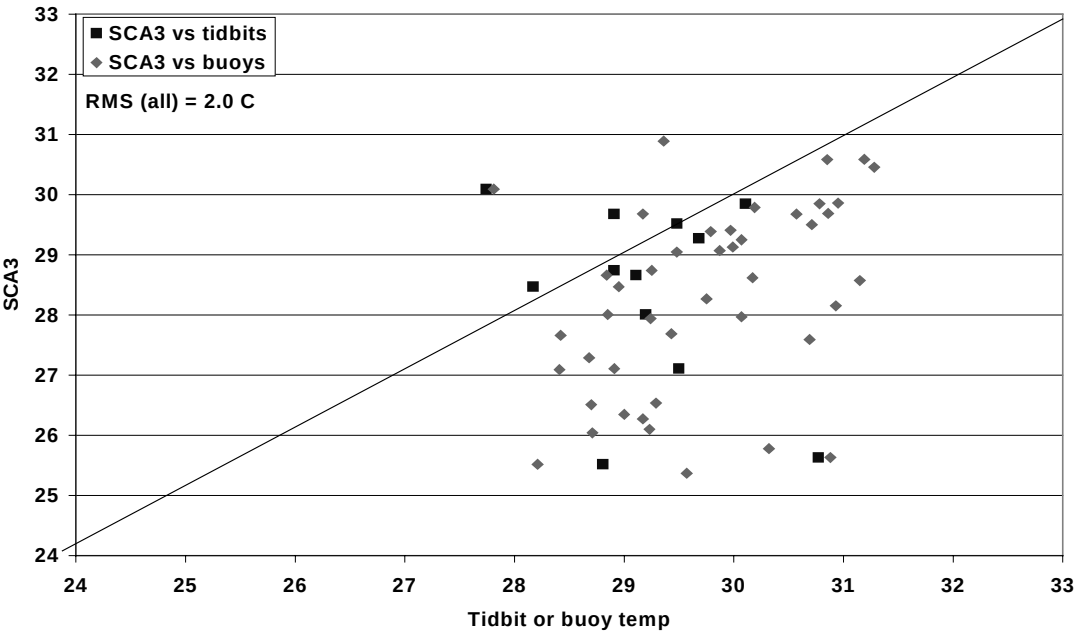

Figure 34. SCA3 temperatures vs. all Tibbit/bouys

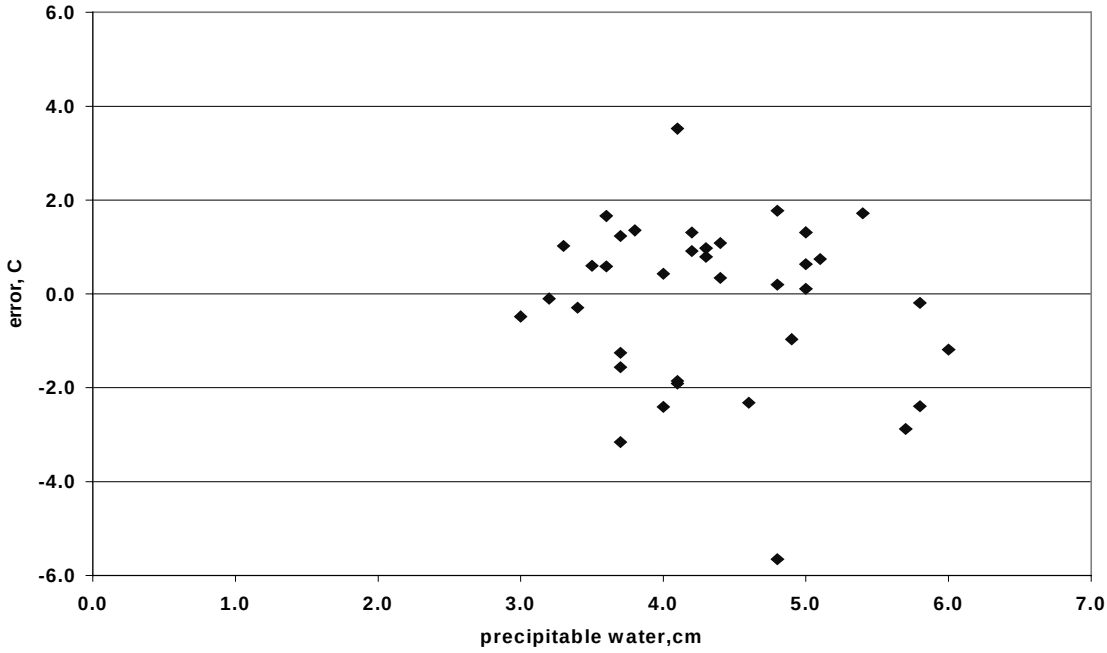

Figure 35. Error in SCA1 vs preciptable water

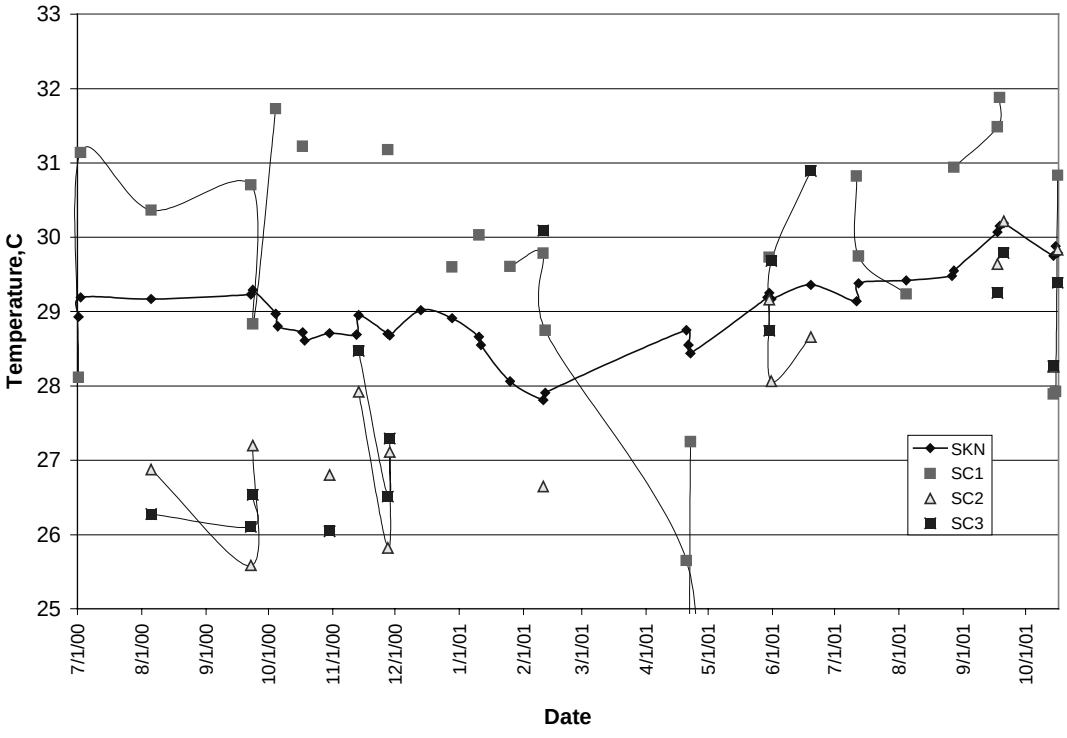

Figure 36. MTI temperatures vs nighttime buoy water surface temperature